DETERMINATION OF SIZE SEGREGATED AEROSOL CONCENTRATION DERIVED FROM AEROSOL OPTICAL DEPTH (AOD) MEASUREMENTS AT VARIOUS LOCATIONS OF DELHI

Dissertation Submitted to the Jawaharlal Nehru University

for the Award of Degree of

MASTER OF PHILOSOPHY

AMIT KUMAR MISHRA

SCHOOL OF ENVIRONMENTAL SCIENCES
JAWAHARLAL NEHRU UNIVERSITY
NEW DELHI - 110 067, INDIA

JULY-2009

जवाहरलाल नेहरू विश्वविद्यालय
Jawaharlal Nehru University
SCHOOL OF ENVIRONMENTAL SCIENCES
New Delhi- 110 067, INDIA

CERTIFICATE

The research work embodied in this dissertation entitled **"Determination of size segregated aerosol concentration derived from aerosol optical depth (AOD) measurements at various locations of Delhi"**, has been carried out at the School of Environmental Sciences, Jawaharlal Nehru University, New Delhi. The work is original and has not been submitted in part or in full, for any other degree or diploma of the university.

AMIT KUMAR MISHRA
(Candidate)

PROF. V. K. JAIN
(Co-Supervisor)

DR. ARUN SRIVASTAVA
(Supervisor)

PROF. K. G. SAXENA
(Dean)

Gram : JAYENU TEL : 26741557, 26742575, 26742676
SES : 26741538 (Direct) 26704302, 4303, 4304 Fax : 26741502

Acknowledgements

I take this opportunity to express my sincere gratitude to Dr. Arun Srivastav, my esteemed supervisor for his keen interest, untiring guidance and for providing constant encouragement throughout the course of the present investigation.

I am deeply indebted to Prof. V. K. Jain, my co-supervisor, for his constant help and for providing the necessary facilities for carrying out this study.

I am thankful to Prof. K. G. Saxena, Dean, School of Environmental Sciences, for providing the necessary facilities. The fellowship provided by the CSIR is gratefully acknowledged.

I wish to express my special thanks to Dr. Sachidanand Singh, National Physical Laboratory, New Delhi, for helping me out with inversion algorithm.

My colleagues from the School of Environmental Sciences supported me in my research work. I want to thank them for all their help, support, interest and valuable inputs. I am especially obliged to Naseer Bhatt, Chander Kumar Singh, Amit Singh and Alok Kumar.

I am thankful to my friends, Luv Kumar, Arvind for their help and encouragement during my field work. My special thanks to my friends, Imran Amin and Kasturi Moitra, who looked closely at the final version of the dissertation for English style and grammar, correcting both and offering suggestions for improvement and also provided moral support during my research work.

Sincere thanks are due to The Chairperson, CSRD, School of Social Sciences for providing me with meteorological data.

Finally, my sincere gratitude to my parents who stood by me throughout my pursuance of this study.

Amit Kumar Mishra

Contents

Certificate

Acknowledgement

List of figures i-ii

List of tables iii

Chapter 1 Introduction 1-10

Chapter 2 Materials & Methods 11-19

Chapter 3 Result and Discussion 20-45

Chapter 4 Conclusion 46-49

References 50-61

List of figures

Fig: 2.1.1	Sampling sites.	11
Fig: 2.2.1	MCROTOPS II Sunphotometer.	14
Fig: 2.2.2	Determination of a and ß by lest squire curve fitting on log-log plot.	17
Fig: 2.2.3	Temporal variation of daily mean relative humidity (RH), temperature, wind speed over JNU.	19
Fig: 3.1.1	Daily spectral variations in AOD observed with MICROTOPS-II Sunphotometer over JNU, Delhi.	21
Fig: 3.1.2	Daily spectral variations in AOD observed with MICROTOPS-II Sunphotometer over Mukherjee Nagar, Delhi.	22
Fig: 3.1.3	Daily spectral variations in AOD observed with MICROTOPS-II Sunphotometer over Patel Nagar, Delhi.	22
Fig: 3.1.4	Daily variation of mean AOD at 500nm.	24
Fig: 3.2.1	Daily variation of wavelength exponent a and turbidity parameter ß.	25
Fig: 3.2.2	Association of a and ß with AOD (500) values over all three sites.	26
Fig: 3.3.1	Diurnal Variation of AOD (500) for different days over JNU.	27-28
Fig: 3.3.2	Diurnal variation of Angstrom wavelength exponent (a) for different days over JNU.	29-30
Fig: 3.3.3	Diurnal association between wave a and AOD (500) for different days over JNU.	31-32
Fig: 3.3.4	Diurnal variation of meteorological parameters (wind speed, wind direction, relative humidity and temperature) for different days over JNU.	33-36
Fig: 3.4.1	Columnar number size distribution of aerosol over JNU, Delhi.	37-38

Fig: 3.4.2	Columnar number size distribution of aerosol over Mukherjee Nagar, Delhi.	39
Fig: 3.4.3	Columnar number size distribution of aerosol over Patel Nagar, Delhi.	40
Fig: 3.4.4	Fine Mode Fraction (FMF) and Coarse Mode Fraction (CMF) in aerosols for different days, over JNU.	42-43
Fig: 3.4.5	FMF and CMF in aerosols for different days, over Mukherjee Nagar.	43
Fig: 3.4.6	FMF and CMF in aerosols for different days, over Patel Nagar.	44
Fig: 3.4.7	FMF and CMF in aerosols for different days, for various days over Delhi.	44

List of tables

Table: 2.1	Specifications of MICROTOPS II Sunphotometer.	13
Table: 3.1	Equation of Number Size Distribution Curve with R^2 values at three observation sites.	41

CHAPTER 1

INTRODUCTION

CHAPTER 1

INTRODUCTION

In today's globalized world, environment is getting a more pervasive attention by the whole world due to the expanding influence of global environmental problems on human life. One of the most prominent environmental problems, climate change by increasing average temperature of earth's atmosphere is a grave concern for developing as well as developed countries due to its sensitivity towards survival of mankind. A common view is that the current global warming rate will continue (Hansen et al., 2000), which is dangerous for our mother earth and her ingredients. Primarily this climate change is a function of composition of atmosphere i.e. greenhouse gases, anthropogenic and natural aerosol, and other constituents of air. As it is a known fact that greenhouse gases (GHGs), since the industrial revolution, play an important role in climate change by warming global atmosphere. Apart from GHGs, aerosols also have the potential to impact the climate, even though the nature of its impact has not yet been clearly established (Charlson et al., 1992). Scientists have much to learn about the way aerosol (directly & indirectly) affect climate.

Most of the scientists believe that aerosol are offsetting 20 to 50 percent of expected global warming that is attributed to increases in the amount of carbon dioxide from anthropogenic activities (Twomey et al., 1984; Charlson et al., 1992; IPCC, 2001). But it does not mean that the aerosol forcing will always counterbalance the greenhouse gases forcing. Meinrat et al. (2005) have pointed out that aerosol forcing will decline relative to GHGs forcing in future because aerosol have shorter life time (5-7 days) in air. In reality, we are still unaware of the sign of aerosol forcing because this information requires the understanding of chemical composition, size and shape of aerosols worldwide. As the characteristics and effects of atmospheric aerosols on climate are still poorly understood, the results of aerosol research are of extreme relevance for contemporary era.

Suspended, solid or liquid, tiny particles in gaseous medium, usually air is termed as aerosol (Reist, 1933; Vincent et al., 1989; Baron et al., 1993). Aerosols are the

mixture of naturally occurring substances, materials introduced into atmosphere by anthropogenic activity as well as the product of gas to particle conversion processes in atmosphere. Human activities, such as burning of fossil fuels and the alteration of natural surface cover, also generate aerosols. Averaged over the globe aerosols, made by human activities currently account for about 10 percent of the total amount of aerosols in our atmosphere. Most of that 10 percent is concentrated in the Northern Hemisphere, especially downwind of industrial sites, slash-and-burn agricultural regions, and overgrazed grasslands. Atmospheric aerosols can be divided into two groups, continental and marine aerosols, on the basis of their genesis. Continental aerosols prominently comprise of wind-blown mineral dust; and carbonaceous and sulphate particles produced by forest fire, land use and industrial activities (Penner, et al., 1994). On the other hand, marine aerosols are mainly sea-salt particles produced by wave-breaking, and sulphate particles formed by the oxidation of dimethyl sulphide released by the phytoplankton (Charlson, et al., 1987). Continental aerosols can be of both, the scattering and absorbing type, whereas marine aerosols are mostly of the scattering type.

Aerosols have significant role in radiative transfer, consequently in the radiation budget. It is also important to mention that one of the most important properties of aerosols used in the radiative transfer calculation is the Aerosol Optical Depth (AOD). AOD is a dimensionless quantity which is defined as the attenuation of direct solar radiation, passing through the atmosphere, by scattering and absorption due to aerosols (Scienfeld et al., 1986). Basically, only the lower few thousand meters of the atmosphere, contribute significantly to the AOD, as aerosol particles mainly originating from the Earth's surface are mixed in this layer of the atmosphere (Alfoldy et al., 2007). Monitoring of AOD at different wavelengths is useful for deriving information about the size segregated aerosol concentration, which in turn helps to identify the source profile of different particles emitted into the atmosphere.

Atmospheric aerosols are of importance because of their impact on human health (Dockery et al., 1993), ability to scatter light; thereby affecting visibility, and their role in global climate change (Scienfeld et al., 1986). These aerosol particles, consisting of complex inorganic and organic compounds, affect the radiation budget, both directly and indirectly. They directly scatter and absorb incoming solar radiation

and out going terrestrial radiation, and indirectly have the ability to modify cloud microphysics and albedo (Charlson et al., 1987).

One of the most important characteristics of aerosols is their particle size distribution. The knowledge of particle size is helpful in understanding dynamics of aerosol-associated atmospheric processes (Marawska et al., 1999). Most importantly, the particle size distribution of aerosols is vital for an accurate and reliable assessment of their impact on human health (Owen et al., 1992; and Fernandez et al., 1999). This is due to the degree of respiratory penetration retention, which is a direct function of the aerodynamic diameter of these particles. It has been found that particles >30 μm in aerodynamic diameter have a low probability of entering the nasal passage of humans. Particles with diameter >5 μm are usually filtered in the nose. Particles with <1-2 μm diameter predominantly get deposited in the alveolar region of the lung during normal breathing (Mc Cornace, 1971). Earlier studies have indicated that the rate of respiratory diseases is considerably higher in urban rather than rural areas. The number of deaths from asthma, bronchitis and emphyserna are significantly related to the concentration of fine respirable particles in the ambient air (Gozmi et al., 1999).

Particle size information is also an important input in models dealing with climate change studies, as radiative forcing of short wave and long wave radiation critically depends on size distribution (Bryson et al., 1967; Tegen et al., 1996). In addition, particle size characteristics of aerosols also affect cloud physics (Haywood et al., 1997; Muller et al., 1999). The existence of modalities in the distribution may help in the identification of aerosol source (Infante et al., 1991). It has been observed that the elements associated with natural resources, such as soil and oceans, are usually found in coarse aerosols, while the elements emitted from anthropogenic sources are associated with fine aerosols (Sceinfeld, 1986).

Numbers of works on aerosol optical properties are being carried out in developed and developing countries due to its health and climate change implications. These works describe various aspects of aerosol optical properties, its diurnal and seasonal variability, and its association with synoptic meteorological conditions.

Schmid et al. (2001) conducted a ground-based measurement with a 6-channel Sun photometer, in which they critically examined the source profile of pollution (long-range aerosol transportation and local source of aerosols). In 2001, Murugavel et al. measured the size distribution of fine aerosol particles of diameter from 0.003 to 1.0 μm were made over the Indian Ocean during IFP-99 of INDOEX. The observation showed a large concentration of aerosols over the Indian Ocean in the Northern Hemisphere, while a lower concentration in the Southern Hemisphere. Tanre et al. (2001) described a novel approach to derive detailed characteristics of aerosol optical properties using a combination of spectral remote sensing from ground based radiometers, and space-borne spectral measurements taken over the Saharan Desert. Esposito et al. (2001) have studied the correlation between ground based measured AOD and TOMS Aerosol Index. In 2002, Dubovik et al., observed a significant variation in absorption for one type of aerosol, due to different meteorological and source characteristics across the world. A seasonal variability of AOD has been observed over the Indian subcontinent using MODIS Data (Prasad et al., 2004). Kedia et al. (2008) have analyzed spatial variations in aerosol optical properties over the Bay of Bengal and Arabian Sea during ICARB cruise period from March to May 2006, using sun photometer and MODIS (Tera & Aqua) satellite measurements. They found a good degree of correlation between sun photometer and MODIS AODs. The AOD was higher in the Bay of Bengal (0.28) than in the Arabian Sea (0.24). Recently, Xie et al. (2008) used satellite based data to asses the extent of aerosol loading in the atmosphere.

Interannual variations in the monthly mean Angstrom wavelength exponent were observed over the Maldives during the north-east monsoon, from 1998 to 2000 (Eck et al., 2001). Formenti et al. (2002) have studied aerosol optical depth and volume size distribution, from spectral measurements of the day time solar extinction and the night time stellar extinction, over a remote semi-arid region of South Africa. During SAFARI 2000, a comparison of aerosol size distribution, radiative properties and optical depths, determined by aircraft observations and sun photometer, was made (Haywood et al., 2003). This comparison showed a consistency between *in-situ* and remotely sensed data, due to the proper mixing of aerosols in the vertical atmospheric column. The aerosol optical properties in the Korea Peninsula, observed at both Kwngju and Anmoyondo during the Asian dust period (March-May), showed a sharp

increase in AOD due to dust storms that frequently occur in this period (Ogunjobi et al., 2003). Microphysical and optical properties of the main aerosol species (ammonium sulphate, nitrate, black carbon, particulate organic matter, sea salt, and mineral aerosol) have been investigated during the ESCOMPTE experiments at a peri-urban site (Mallet et al., 2003). In another experiment over Kwangju, Ogunjobi et al. (2004) observed that the optical depth showed a pronounced temporal trend. They also found that the maximum dust loading was observed during spring time and biomass-burning aerosols were observed in early summer and autumn. Recently, in a similar type of work significant temporal trend of AOD, with maximum aerosol loading during December-March period in Sub-Saharan West Africa (Ogunjobi, 2007) was reported.

Widespread measurements of turbidity parameters have been carried out in the past at different Indian locations using single- and three-wavelength Volz sunphotometers (Mani et al., 1969). Krishnamoorthy et al. (1988), conducted a study at Trivandrum (India) in 1984 using three narrow-band filters, which exposed several aspects of aerosol extinction features. A network of Multi-Wavelength Radiometer (MWR) stations was set up at different locations to cover different types of environments; e.g., rural, urban, coastal, marine, arid, desert, etc. A brief assessment of the scientific results obtained from these stations was reported by Subbaraya et al. (2000). Many other experiments, clearly demonstrating the importance of the impact of absorbing aerosols on the radiation budget across India, were carried out in the early years of this decade (Ramanathan et al., 2001; Satheesh et al., 2002; Sumanth et al., 2004). In order to provide a comprehensive characterization of the spatial and temporal variations in the physical, chemical and radiative properties of aerosols, experiments over the Arabian Sea region under ISRO-Geosphere Biosphere Programme (ISRO-GBP) have recently been conducted (Satheesh et al., 2006).

The aerosol optical properties are very much dependant on regional weather parameters such as wind speed, wind direction, relative humidity (RH), temperature etc. Sinirnov et al. (2003) have shown the effect of wind speed on AOD, Angstrom wavelength exponent and size distribution over the Midway Island. Aoki and Fujiyoshi (2003) computed aerosol optical depths, Angstrom wavelength exponent and volume size distribution within an atmospheric column, using ground based sky-

radiometers over Japan. They described the seasonal variability in the above properties and characterized aerosol types on the basis of measured AODs. The association between size segregated, near-surface aerosol mass concentration (measured by Quartz Crystal Microbalance Impactor: QCM) and aerosol optical depth (using Multi Wavelength solar Radiometer: MWR) has been examined in the past (Pillai et al., 2004). Yoon et al. (2006) have investigated the influence of relative humidity on aerosol optical properties and aerosol radiative forcing. They found that AOD at 550 nm, increased to factor 1.24, 1.51, 2.16 and 3.20, at different RH levels of 70, 80, 90 and 95%, respectively, due to hygroscopic growth of aerosol particles. Sarkar et al. (2006) have discussed the analysis of the temporal and spatial variation in aerosol properties and aerosol forcing, for major populated and industrial cities (Delhi, Kanpur, Chandigarh, Lucknow, Kolkata, Ahmedabad, Mumbai and Jaipur) in India. The results clearly showed that AOD over the northern part of India is higher as compared to the southern part. Moreover, related experiments have been done in India, which showed a good association of AOD and particulate matter mass loading, with the wind direction (Kharol et al., 2007). Some researchers have estimated spectral aerosol optical depth using MICROTOPS-II Sun photometers over Rajkot (Ranjan et al., 2007). The measured aerosol optical depth showed seasonal variation, with high values in summer and low values in winter. Adamopoulos et al. (2007) studied the aerosol particle sizes retrieved from solar spectral measurements in the ambient air of Athens in Greece. In this study, the largest particles were observed in summer and the smallest during winter. Similarly Parsiani et al. (2008) carried out, Sun-photometer aerosol optical depth data and Artificial Neural Network study for accurate prediction of aerosol size distribution (ASD) function.

Retrieval of aerosol size distribution from aerosol optical depth has been carried out by many scientists across the world. At present, several techniques are in use for reconstructing size distribution from experimental data of extinction coefficient and scattering measurements. These techniques have certain deficiencies. In fact it is doubtful if there is any method that can perfectly reconstruct aerosol size distribution from a limited set of data. Various studies on inversion algorithm using spectral extinction and optical scattering measurements, to retrieve aerosol properties (such as aerosol size distribution) in past few decades are as follows:

A relationship between the size of atmospheric aerosol particles and the wavelength dependence of the extinction coefficient was first suggested by Angstrom (1929). Yamamoto and Tanaka (1969) were the first to apply a numerical inversion algorithm to spectral measurements of extinction coefficient, in order to determine aerosol size distribution. These authors applied the linear inversion techniques developed by Phillips (1962) and Twomey (1963) to the problem enconterde while numerically solving the Fredholm integral equation of the first kind. King et al. (1978) have proposed a numerical inversion algorithm to retrieve columnar aerosol size distribution using particulate optical depth as a function of wavelength. They found three distinctly different categories of size distribution of aerosol particles. Approximately 50% of the distribution represented both, Junge (Power law) distribution and a distribution of relatively mono-dispersed large particles; 20% of the distribution yielded only Junge size distribution; while 30% yielded only a relatively mono-dispersed distribution. The technique of recovering the particle size distribution function by combining measurements of scattered radiation and Spectral extinction has been discussed earlier (Shaw, 1979). Crump and Seinfeld (1981) have discussed the inversion problem that arises while retrieving aerosol size distribution and showed the shortcomings of the methods used at that time. They have suggested the method of generalized cross validation as an alternative.

In the development of linear inversion technique, Hagen and Alofs (1983) presented a linear inversion method to perform aerosol size distribution for differential mobility analyzer measurements. This method showed a good immunity to both random and systematic experimental error. Markowski (1987) improved Twomey's algorithm (1975) for inversion of aerosol measurement data. Twomey's algorithm has been widely used, but its results depend, to some extent, on the initial guess, and often producing oscillatory results. Intelligent guesses made, along with further smoothening of the Twomey's algorithm, greatly increased the quality of the inversion results obtained. Kaufman et al. (1994) used the retrieval procedure of Nakajima et al. (1983) to determine size distribution and the scattering phase function acquired in several geographical locations having different aerosol types.

In the mid 1990s, many developments were made in the inversion technique for *in situ* or ground based remote sensing measurements of optical data (both spectral extinction and scattering data). An inversion technique based on angular dissymmetry to determine the size distribution of a non-absorbing aerosol has been developed by Chang et al. (1995). They extended the technique developed for obtaining the size distribution of a single component aerosol (Chang and Biswas, 1992) to a multi-component system. Amato et al. (1995) have inverted grating spectrometer measured AOD to determine the size distribution of atmospheric aerosols. They used Phillips-Twomey inversion method along with suitable selection of regularization parameter. Wang et al. (1996) investigated the retrieval of aerosol size distribution from simulated aerosol-extinction-coefficient measurements of the satellite instrument during the stratospheric aerosol and gas experiment (SAGE-III). Their results procured unimodal as well as bimodal size distributions using randomized minimization search technique and the optimal estimation theory.

In the wake of the twenty first century, an algorithm to retrieve aerosol optical properties and size distribution from ground based sun-sky radiance measurement has been developed, by means of including a detailed statistical optimization of measurement variance in the inversion procedure (Dubovik and King, 2000). A novel inversion technique to determine the particle size distribution and sample concentration from spectral measurements using evolutionary programming, has been developed for the two cases of known and unknown relative refractive indices (Li and Wilkinson, 2001). Paganini et al. (2001) used an instrument to obtain long path extinction measurements for sizing of air borne particles, in which a non-linear iterating algorithm (Ferri et al., 1995) was used for inversion.

Factually speaking, the traditional inversion method for spectral extinction such as the direct inversion method and non-liner iterative inversion method were time consuming and also unsatisfactory in some cases. For improving results of size distribution, Li et al. (2001) used neural networks for determining particle size distribution from spectral extinction measurement. Compared to the established methods of inverting the Fredholm integral equation, neural network supply solutions were essentially instantaneous and did not need an empirical parameter. Kobayashi et al. (2006) rewrote the software (SKYRAD.pack, 1996) by applying the statistical

optimization method to its inversion algorithm, thereby making it easier to improve and extending its analytical capabilities in future. Recently Sun et al. (2007) studied particle size range in the visible spectrum with a primary focus on forward scattering correction in spectral extinction inversion. The particle size distributions were retrieved in both the dependent and independent models. They found that the particle size distribution could be retrieved very well for sizes ranging from 0.1 μm to 12 μm.

Although many works have been done on aerosol properties, such as aerosol radiative forcing and its size distribution, chemical characterization and source apportionment etc. over Delhi (Singh et al., 2005; Srivastava and Jain, 2003, 2005, 2007a, b, c, 2008), the application of aerosol optical depth measurements to determine aerosol size distribution is relatively new for Delhi.

In the present study aerosol optical depth (AOD) measurements using MICROTOPS II Sunphotometer in 380-1020 nm wavelength range have been carried out, at three different locations of Delhi, viz: Jawaharlal Nehru University (25 Feb-6 March), Mukherjee Nagar (5-12 May) and Patel Nagar (13-15 May). Everyday measurements were taken at 15 or 20 minutes interval, from morning to evening. We have used King et al. (1978) inversion algorithm to determine size segregated aerosol concentration over Delhi because it gives a positively constrained result and is easy to use. However this inversion algorithm is also one of the basic pillars in the field of inversion procedure. We have taken a complex refractive index of aerosol m = 1.45+0.0002*i*, which is assumed to be independent of size and wavelength. The value lies somewhere within the mixed aerosol particle range (Yamamoto and Tanaka, 1969). The limits of radius range of maximum have been used as $0.1 \leq r \leq 7.8$ μm, in this study.

The objectives of present study are as follows.

1. A comprehensive analysis of daily spectral variation of aerosol optical depth (AOD) on observed days, over three location of Delhi.

2. An analysis of daily variation in Angstrom wavelength exponent (α) and turbidity coefficient (β) over all three locations of Delhi.

3. A comparison of diurnal variation in AOD (500) and Angstrom wavelength exponent (a), and their association with synoptical meteorological conditions.

4. Determination of size segregated aerosol concentration using AOD measurements.

5. Determination of the fine mode fraction (FMF) and coarse mode fraction (CMF), using columnar aerosol size distribution curves for each day of measurements over Delhi.

The dissertation is divided into four chapters. A description of the study area, experimental design and methodology is given in chapter 2. The result and discussion is described in chapter 3. Finally the conclusions drawn from the study are presented at the end in chapter 4.

CHAPTER 2

MATERIALS AND METHODS

CHAPTER 2

MATERIALS AND METHODS

2.1 STUDY AREA

The present study pertains to Delhi, the capital city of India. It lies 160 kms south of the Himalayan Mountains, between the latitude 28.21' to 28.53' and longitude 76.20' to 76.37'. It is 213.3 to 305.4 m above the sea level. The climate of Delhi is mainly influenced by the prevalence of continental air for a major part of the year. Extreme dryness owing to intense dry air and cold winters are the main climatic characteristics of Delhi. The city receives an average amount of rainfall of approximately 611.8 mm. Winds blow from the western direction but tend to be more northerly in the afternoon. Easterlies and south easterlies are most common in the monsoon months (July to August). While February and March correspond with the spring season, May and June are the hottest months of the year with temperature soaring up to 46 to 49 ^{0}C.

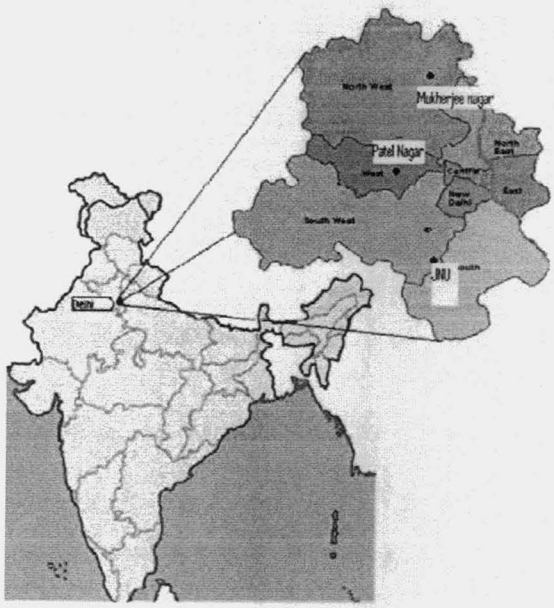

Fig: 2.1.1 Sampling sites [Not to scale]

SAMPLING SITES

The aerosol optical depth measurements were taken using ground based sun photometer at three different sites (shown in Fig: 1) whose descriptions are as follows.

JNU

Jawaharlal Nehru University (JNU) campus, far from any industrial activity, is situated in the southern outskirts of Delhi. Even though it has low vehicular traffic, ongoing construction work for new school buildings and hostels during the period of observation, has contributed to the suspended particles in the surrounding air. Apart from residential and academic areas for students and faculties, it also has many *dhabas* (canteens) and hostel messes which can be a source of carbonaceous aerosols. The campus is replete with green vegetation which sets it apart from the other two areas that have been taken up in this study.

MUKHERJEE NAGAR

Dr. Mukherjee Nagar is along the northern outskirts of Delhi. Being close to the Delhi University, the area has a robust student population living here. However, the fact that it has Delhi ring road, NH1 bypass (to Amritsar) and Wazirabad road nearby, which add vehicular traffic emissions to exiting aerosol particles in the area. This can be compared and contrasted with JNU, the other student dominated area under study.

PATEL NAGAR

Patel Nagar is situated more or less at the centre of the city. There are some small scale industries like blacksmiths, carpentry and furniture, clothing's etc. in the adjoining areas of Karol Bagh, Sadar Bazar. Its location alongside a heavy intersection of traffic coming through Shankar Road, Farm side Road, Old Rohtak Road, Naraina Marg and Shivaji Marg adds a distinct character to aerosols from the region. Therefore, this site presents a far more different picture as compared to the other two sites.

2.2 INSTRUMENTATION AND DATA ANALYSIS

Measurement of aerosol optical depth and columnar water vapour was carried out using a Sunphotometer, the MICROTOPS II of the Solar Light Company Inc, USA

(figure:2). The Sunphotometer measures the direct solar radiations of five different wavelength (380, 500, 675, 936, and 1020 nm) using a narrow band of interference filters. Complete details of the instrument and measurement techniques can be found in User Guide, MICROTOPS II Sunphotometer version 5.5, Solar Light Company Inc. The specification of the instruments is shown in the following chart.

Table: 2.1 Specifications of MICROTOPS II Sunphotometer

Total Optical Channels of Sunphotometer	340 ± 0.3 nm, 2 nm FWHM *380 ± 0.4 nm, 4 nm FWHM 440 ± 1.5 nm, 10 nm FWHM *500 ± 1.5 nm, 10 nm FWHM *675 ± 1.5 nm, 10 nm FWHM 870 ± 1.5 nm, 10 nm FWHM *936 ± 1.5 nm, 10 nm FWHM *1020 ± 1.5 nm, 10 nm FWHM ***These were the channels calibrated in sun photometer for our studies.**
Max. out-of-bond sensitivity, Relative to peak transmission	340nm: 1E-6 λ<650nm; 1E-5 λ<1.0μm 380nm: 1E-6 λ<650nm; 1E-5 λ<1.0μm 440nm: 1E-5 λ<1.0μm 500nm: 1E-6 λ<1.1μm; 1E-5 λ<1.2μm 675nm: 1E-6 λ<1.1μm; 1E-5 λ<1.2μm 870nm: 1E-6 λ<1.1μm; 1E-5 λ<1.2μm 936nm: 1E-6 λ<1.1μm; 1E-5 λ<1.2μm 1020nm: 1E-6 λ<1.1nm; 1E-5 λ<1.2μm
Resolution	0.1W/m²
Dynamic range	>300,000
Angle of view	2.5°
Precision	1-2%
Non linearity	Max. 0.002%
Operating environment	0 to 50°C, no precipitation
Computer interface	RS-232C
Power source	4xAA Alkaline batteries
Weight	21 oz (600 grams)
Size	4"W x 8"H x 1.7"D (10x20x4.3 cm)

Fig: 2.2.1 MCROTOPS II Sunphotometer

2.2.1 THEORY OF SUNPHOTOMETER

Solar irradiance transmittance can be calculated with the Beer – Bouguer – Lambert law:

$$I = I_0 \exp(-\tau m) \qquad (1)$$

Where I_0 is the spectral irradiance value outside the atmosphere, τ is the total optical depth of the atmosphere and m is the optical mass defined as the ratio between the vertical optical total depth and the optical depth in a specific direction (Iqbal, M., 1983).

Eq. (1) can be rearranged using voltages instead of irradiance:

$$V = V_0 \exp(-\tau m) \qquad (2)$$

In order to know the optical mass, it is convenient to assume the atmosphere to be plane (not spherical), which makes it possible to write this parameter as a function of solar zenith angle (θ) as,

$$m = 1/\cos(\theta) \qquad (3)$$

Nevertheless, because of the Earth's curvature, refraction in air and multiple scattering, Eq. (3) fails beyond 60 degrees of solar zenith angle. So, it is a better approximation to use other empirical equations like Kasten's (1966):

$$m = 1/ [\cos\theta + 0.50572 (1.46468- \theta)^{-1.6364}] \quad (4)$$

where θ is the solar zenith angle (in radians). From the Beer–Bouguer–Lambert law, the total optical depth of the atmosphere is given by:

$$\tau = - (1/m). \ln (I/I_0) \quad (5)$$

The aerosol optical depth (AOD) is the main parameter in the study of the aerosol properties. It is an indicator of the vertical content of concentration of aerosols in the atmosphere. Since, the measuring range does not cover the other contribution like Rayleigh particles and gases; therefore, τ represents the AOD in present Sunphotometer.

The Sunphotometer was calibrated using Langley method which is based on Beer-Bougher-Lambert law. Since measurements are obtained for each wavelength, it is specified on the corresponding equation as a λ subscript, so:

$$I_\lambda = I_{0\lambda} \exp (- \tau_\lambda m) \quad (6)$$

where I_λ is the irradiance measured at ground level, $I_{0\lambda}$ the extraterrestrial irradiance, corrected from the earth-sun distance, τ_λ is total optical depth of the atmosphere and m is the optical mass. From this equation we have that:

$$\ln(I_\lambda) = \ln(I_{0\lambda}) - \tau_\lambda m \quad (7)$$

Now, if we keep total optical depth constant and the logarithm of measured irradiance is represented against the optical mass for a certain wavelength along a series of measurements, the result is a straight line whose slope is (as it is indicated in the equation) the total optical depth, and the ordinate at the origin corresponds to the

extraterrestrial irradiance for that wavelength or channel. This value will give us the calibrating coefficient for that specific wavelength or channel. If the extraterrestrial signal (in voltage or digital counts) and the extraterrestrial irradiance spectrum are compared, calibrating coefficients can be obtained to convert raw signal into physical units. These coefficients, as they are obtained from Langley fit, depend on the earth-sun distance.

The initial hypothesis to calibrate is that the total optical depth is kept constant; in fact, the ideal conditions to perform a Langley calibration require a minimal variation in the total optical depth. These variations usually appear because of aerosols; thus, in order to obtain the least variation in this parameter, places having low amounts of aerosol are sought where their variations are few in absolute terms. Stations above the limit layer are the most suitable for these calibrations.

2.2.2 DETERMINATION OF ANGSTROM PARAMETER

The spectral dependence of aerosol optical depth (AOD) can be analyzed using the Angstrom's formula (Angstrom, 1961), which states that extinction of solar radiation by aerosol is a continuous function of wavelength, without selecting the bonds for scattering or absorption. Thus, the formula derived is empirically given as,

$$\tau_\lambda = \beta \lambda^{-\alpha} \qquad (8)$$

where, τ_λ is the aerosol optical depth at wavelength (λ, μm), β is the turbidity coefficient and α is the wavelength exponent. Cachaorro et al. (2000) have shown that angstrom formula provides a good spectral representation of the atmospheric aerosol attenuation. The wavelength exponent depends on the size distribution parameters of aerosol while the turbidity coefficient is directly proportional to the columnar aerosol content and is equal to the AOD measured at 1 μm. Large value of α indicates a relatively high ratio of small to large particles. When α approaches 4, it indicates the presence of very small aerosol particles (on the order of air molecule) whereas $\alpha \approx 0$ represents very large particles (Hoblen et al., 2001; Pinkar et al., 2001).

For the purpose of determining α and β values by the linear regression, the above equation (8) can be expressed in the form:

$$\ln\tau_\lambda = \ln\beta - \alpha\,\lambda \qquad (9)$$

So we can evaluate α and β by the least square linear curve fitting on the log-log plot. The slopes of the graphs provide the wavelength exponent α and its intercept lnβ. Figure: 3 show the calculation of α and β on 25 Feb, 02 Mar, 06 May and 14 May.

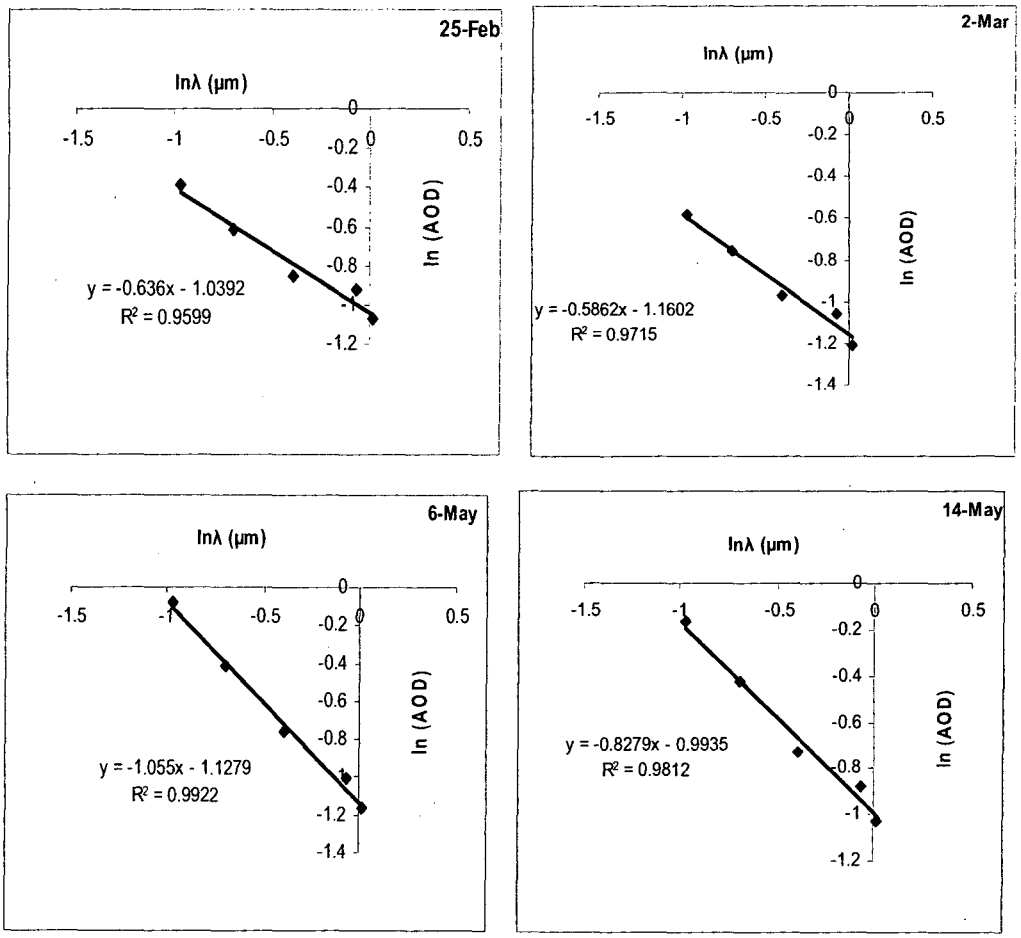

Fig: 2.2.2 Determination of α and β by lest squire curve fitting on log-log plot

2.2.3 INVERSION OF AOD

The columnar aerosol size distribution is derived from aerosol optical depth (AOD) by numerical inversion of the Mie Integral (King et al., 1978). The Mie integral

$$\tau_\lambda = \int \pi r^2 Q_{ext} (m, r, \lambda) n_c (r) dr \qquad (10)$$

represents the relation between spectral dependence of the aerosol optical depth and columnar size distribution function where, Q_{ext} is the aerosol extinction efficiency factor which depends on aerosol refractive index (m), radius (r) and the wavelength (λ) of the incident radiation. n_c (r) is the columnar size distribution function of the aerosol. A moderate refractive index value of 1.45+0.0002i (chapter 1) was used for this inversion calculation.

2.2.4 METEOROLOGICAL DATA

The meteorological Parameters for JNU site were collected from CSRD, SSS I, JNU, New Delhi (100 meters from the observation site). The daily variation in temperature, relative humidity and wind speed are shown in Fig: 2.2.3.

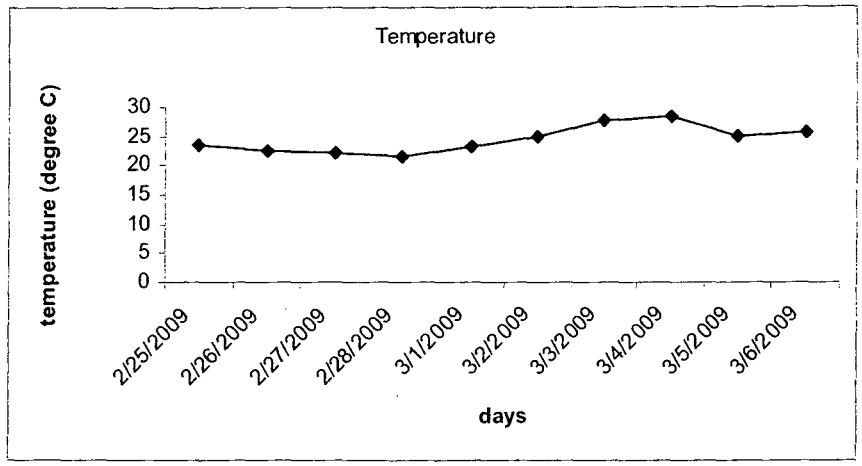

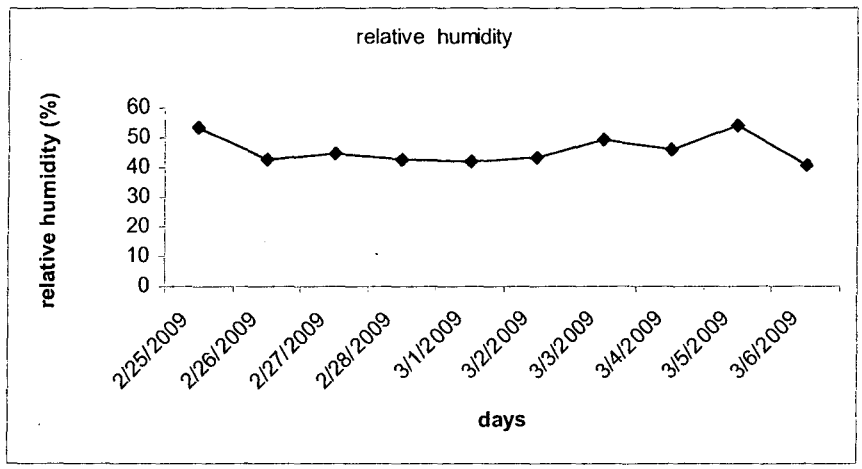

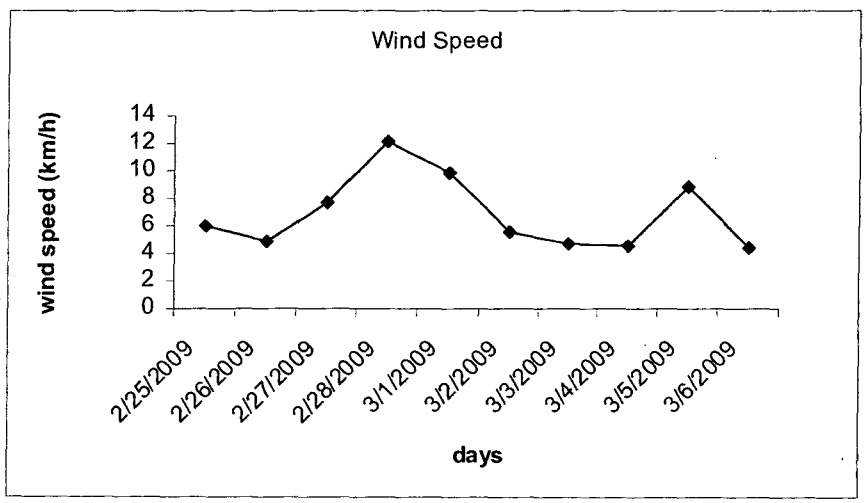

Fig: 2.2.3 temporal variation of daily mean relative humidity (RH), temperature, wind speed over JNU

CHAPTER 3

RESULT AND DISCUSSION

CHAPTER 3

RESULT AND DISCUSSION

3.1 Daily spectral variation of AOD

It is necessary to know the spectral dependence of AOD to retrieve other aerosol optical parameters from ground based or satellite based remote sensing measurements (Eck et al., 1999). The wavelength dependence of AOD varies with different aerosol type due to its different physical and chemical properties. Fig: 3.1.1, 3.1.2, & 3.1.3 show daily variation of AOD in 380nm – 1020nm wavelength range for various days at three different places of Delhi, viz: Jawaharlal Nehru University (JNU), Mukherjee Nagar, and Patel Nagar respectively. The standard deviation of AOD at each wavelength has also been represented as vertical line (error bar) on the plot itself.

The spectral variation of columnar AOD, observed on different days, over all three sites, indicates a systematic spectral dependence according to classical Mie scattering theory. It can easily be inferred from these figures that there are significant variations in spectral dependence of AOD at all three different sites. It is evident from the figures that there is relatively strong spectral dependence of optical depth at shorter wavelengths (steeper slope) than longer wavelengths (gentler slope). However, the magnitude of AOD decreases with increase in wavelength on each days of observation (except 4^{th} and 10^{th} May). This is an indication of the presence of smaller to larger particle size distribution (Srivastava et al, 2008). The higher concentration of the fine mode particles, which are selective scatters, enhances the irradiance scattering, and therefore, the AOD values are high at shorter wavelengths. Likewise, the coarse mode particles provide similar contribution to the AOD at both, shorter and longer wavelengths (Schuster et al., 2006).

Fig: 3.1.1 (h) and 3.1.2 (d) show a different picture of spectral dependence of AOD as compared to other days. The spectral variation of AOD exhibits high AOD at smaller wavelengths and vice-versa (similar to other days), except a slight enhancement in AOD at 936 nm, which may be due to interference of a weak water vapour absorption band (Dani et al., 2003). This result reveals the presence of optically thin sub-visible cloud/haze layers in sensing region, on 4^{th} Mar and 10^{th} May.

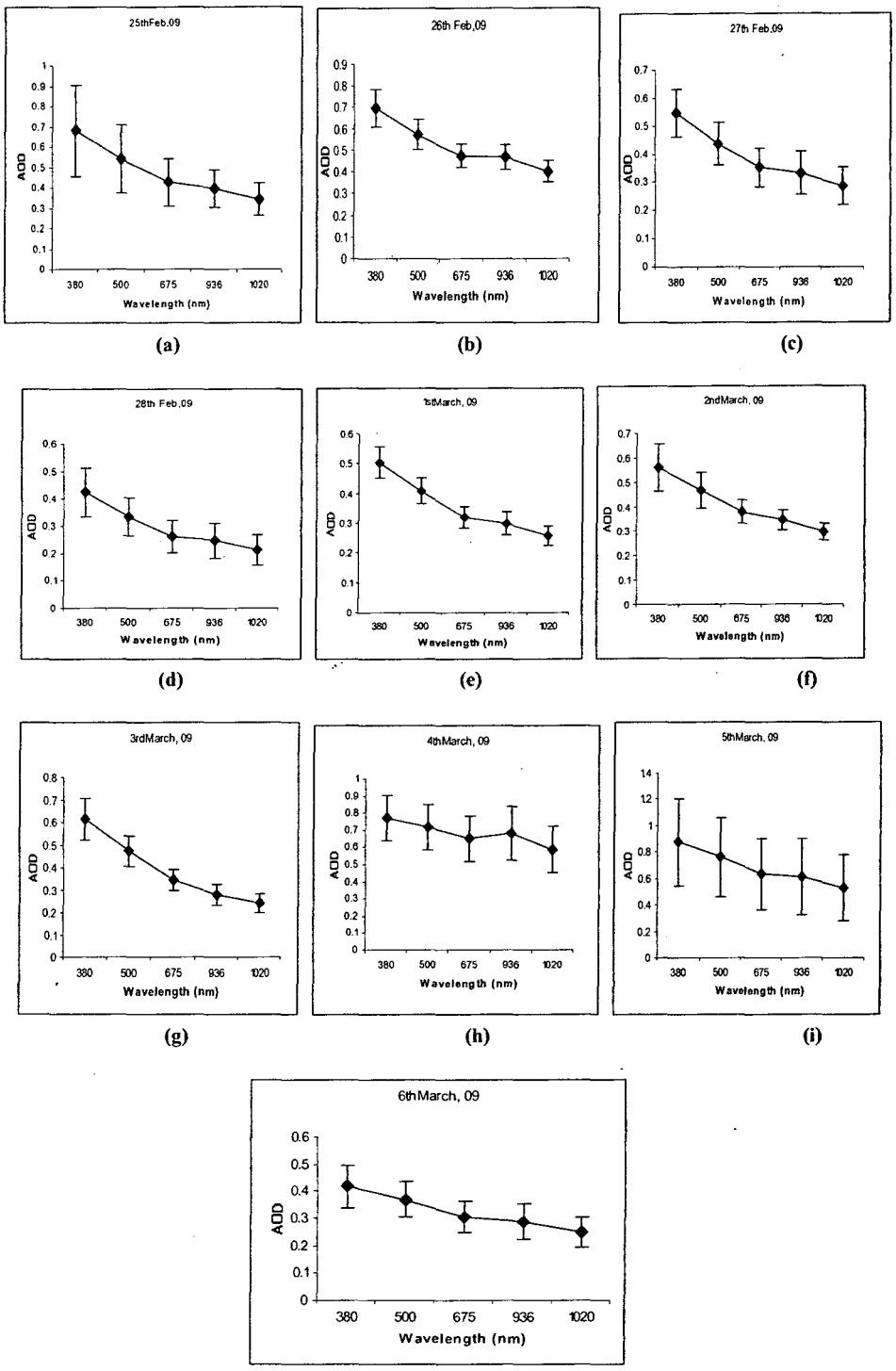

Fig: 3.1.1 Daily spectral variations in AOD observed with MICROTOPS-II Sunphotometer over JNU, Delhi.

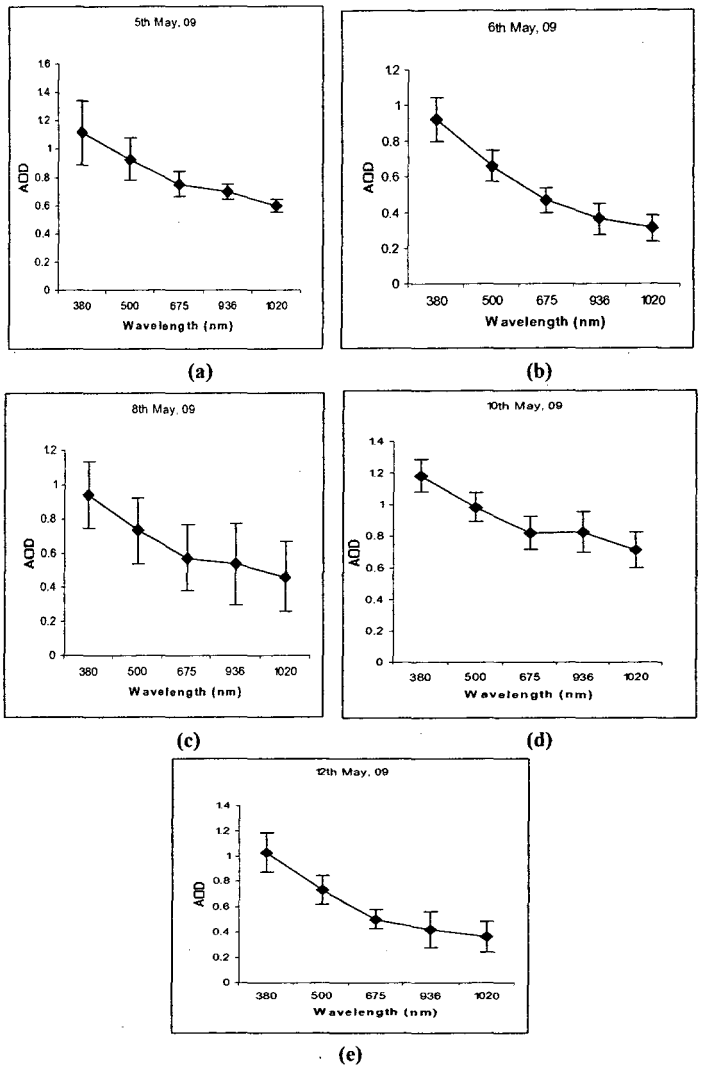

Fig: 3.1.2 Daily spectral variations in AOD observed with MICROTOPS-II Sunphotometer over Mukherjee Nagar, Delhi.

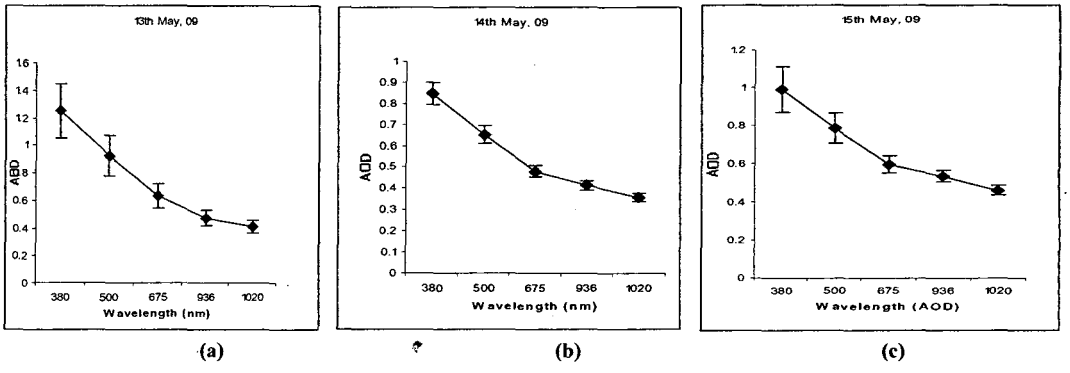

Fig: 3.1.3 Daily spectral variations in AOD observed with MICROTOPS-II Sunphotometer over Patel Nagar, Delhi.

An interesting feature observed from Fig: 3.1.1, 3.1.2 and 3.1.3 that the standard deviation of AOD at each wavelength decreases towards higher wavelengths, which

shows the sensitivity of AOD measurements at lower wavelengths in visible region. Relatively high standard deviation at all wavelengths, on 4th, 5th March (JNU) and 8th May (Mukherjee Nagar) attributed to pronounced diurnal variation in concentration of both, fine and coarse aerosol particles.

The magnitudes of AOD, at all wavelengths, are significantly higher over Mukherjee Nagar and Patel Nagar as compared to JNU (Fig: 3.1.1, 3.1.2, 3.1.3). This may be attributed to the fact that JNU is located far away from any industrial activities as compared to other two observed site which have higher AOD values. It is also clear from Fig: 3.1.4 that the magnitude of AOD values increase as month progress from March to May due to continuous increase in dust loading in the atmosphere, from March to May. This is in conformity with Sumita et al. (2008).

From figure 3.1.4, it can be easily inferred that the AOD (500) shows lower values in weekends (28th Feb, 1St March), over JNU as compared to week days. However these types of observation were not observed over the other two sites. This result may be attributed to major dust and haze events in the month of May over Delhi.

Over JNU during 25 Feb-6 March, the magnitude of AOD (at 500 nm) values are in the range of 0.33 to 0.76, whereas, Mukherjee Nagar and Patel Nagar, during 5-15 May, show high values of AOD (at 500 nm) in the range of 0.65 to 0.98 (Fig: 3.1.4). This result shows a good agreement with the fact that dust activity is found to peak in Indian subcontinent, during spring (March to May), and decreases with the onset of southwest monsoon (Prospero et al., 2002). Also during May, mostly, southerly winds carry dust particles from Rajasthan side (Sikka, 1997) leading to hazy conditions.

Over JNU, 4th and 5th March show higher AOD (500) (0.71 and 0.76 respectively) values as compared to other days. This result shows high aerosol loading on these two days, either due to local anthropogenic activities or long range transportation of polluted aerosols. Over Mukherjee Nagar and Patel Nagar, relatively higher AOD (500) on 5th, 10th, and 13th May (0.92, 0.98 and 0.91 respectively) attributed to presence of haze layers during observation. This results show a good consistency with Gupta et al. (2005) results over Delhi.

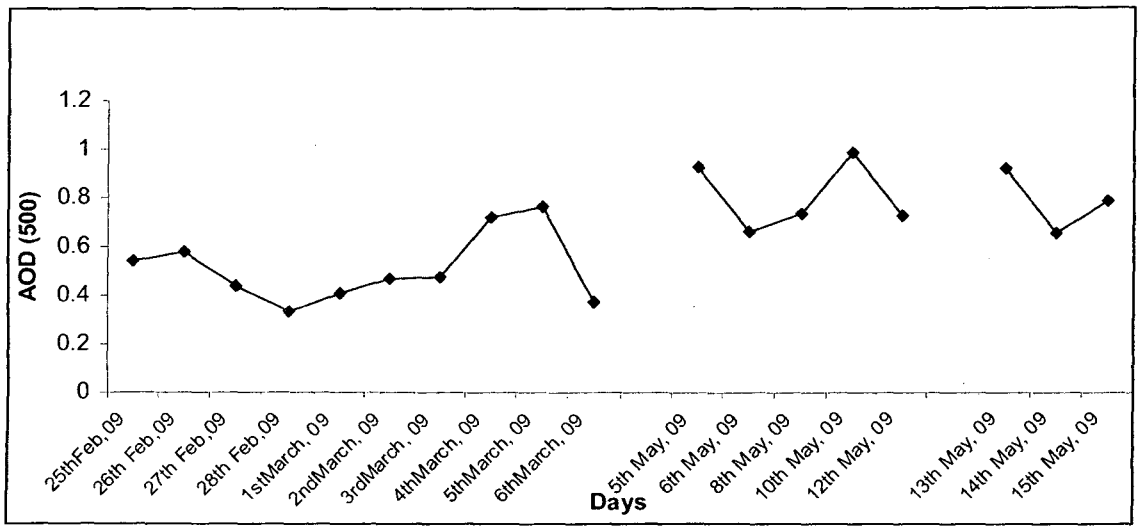

Fig: 3.1.4 Daily variation of mean AOD at 500nm.

3.2 Daily variation of Angstrom wavelength exponent (α) and turbidity coefficient (β)

Cacharro et al. (2000), showed that Angstrom formula ($\tau_\lambda = \beta\lambda^{-\alpha}$; Chapter 2) provides a good spectral representation of atmospheric aerosol attenuation. The wavelength exponent α is an index for the aerosol size distribution and depends on the ratio of the concentration of small to large aerosol (Shifrin, 1995), while the turbidity coefficient β represents the aerosol concentration present in vertical column. The wavelength exponent α and turbidity parameter β computed for each day over all three sites is plotted in Fig: 3.2.1.

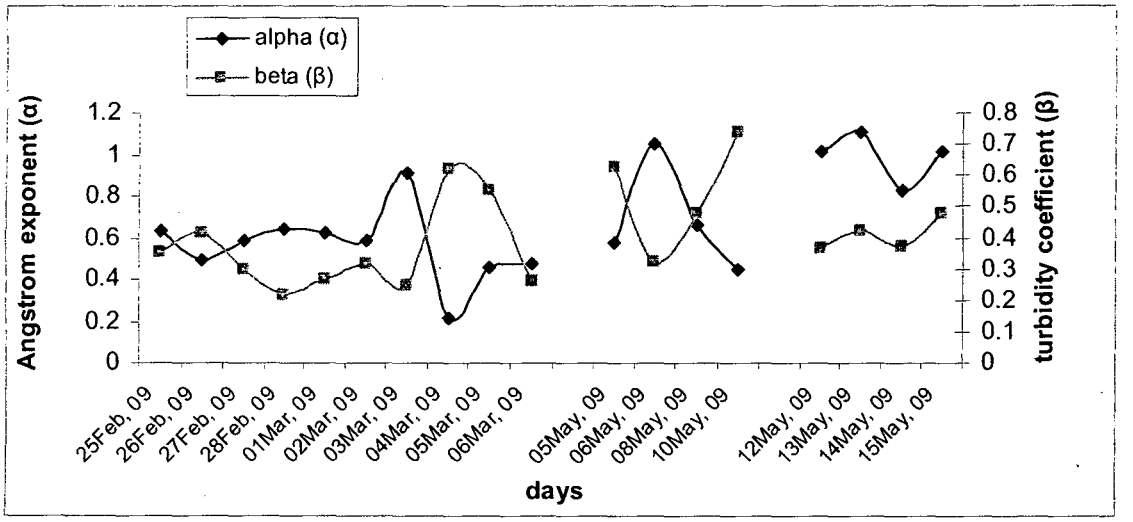

Fig: 3.2.1 Daily variation of wavelength exponent α and turbidity parameter β

Our data reveal an inverse relationship between wavelength exponent α and turbidity parameter β values i.e. the high α values associated with the low β values and vice-versa, over all sites, except Patel Nagar. The inverse relationship between α and β agrees with earlier observations by Adeyewa and Balogun (2003), Dani et al. (2003), Sateesh et al. (2006) and Ranjan et al. (2007).

Fig: 3.2.2 shows that a good association of α and β with AOD (500) values. Normally turbidity parameter β increases with increasing AOD (500) values and vice-versa, whereas, wavelength exponent α decreases with increasing AOD (500) values and vice-versa (except over Patel Nagar). Both α and β show similar pattern with AOD

(500) over Patel Nagar i.e. increases with increase in AOD (500) values and vice-versa.

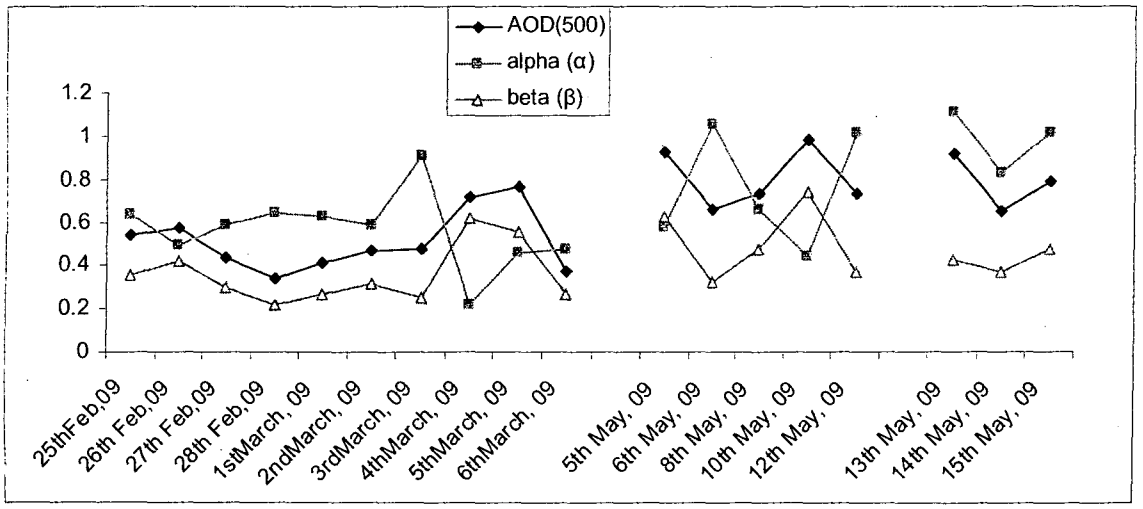

Fig: 3.2.2 Association of α and β with AOD (500) values over all three sites

However, the Daily variation of α and β do not show any definite pattern over any site, which attributed to high variation in Daily synoptical meteorological parameter and aerosol loading over study area.

Relatively higher value of α, over Patel Nagar (0.82-1.11) and Mukherjee Nagar (0.44-1.05) than JNU (0.2-0.9), indicated the presence of relatively finer mode aerosol particles than coarse mode, over Patel Nagar and Mukherjee Nagar. The higher values of wavelength exponent α on 3rd March (0.91), 6th May (1.05), 12th May (1.01), 13th May (1.11) and 15th May (1.01) indicate the low concentration of coarse mode aerosol particles as compared to other days of observation.

Higher values of β on 4th March (0.61), 5th May (0.62) and 10th May (0.74) show relatively higher aerosol loading on these days as compared to other days. Whereas, low values of β over JNU (0.26-0.41) except 4th and 5th Mar, shows relatively low columnar aerosol mass loading than Mukherjee Nagar (0.32-0.74) and Patel Nagar (0.37-0.47).

3.3 Diurnal variation of AOD (500) and Angstrom wavelength exponent (α), and their association with synoptical meteorological condition

The analysis of diurnal variation of AOD (500) and wavelength exponent and their association with meteorological parameter has been done over JNU site only, due to continuous data measurement from morning to evening, at every 15 minute interval. Also the diurnal meteorological parameters were recorded in proximity of the study point (about 100mts away).

Fig: 3.3.1 shows the diurnal variation of AOD (500) for different days over JNU. Approximately all days show relative high AOD (500) during 10 am to 12 pm and 2 pm to 3 pm except weekends. The high AOD (500) during 10 am to 12 pm and 2 pm to 3 pm may be attributed to morning office traffic rush hour (vehicular pollution) and school closing times (which also leads to vehicular emission) respectively. However, 28th Feb (Saturday) shows relatively high AOD (500) range during 12:30pm to 2:30 pm which may be attributed to high vehicular emission due to half working days on Saturday. Where as 1st march (Sunday) show relatively high AOD (500) in the afternoon, attributed to the relatively high vehicular emission caused by people going for their weekly outings on Sunday afternoon (Fig: 3.3.1b).

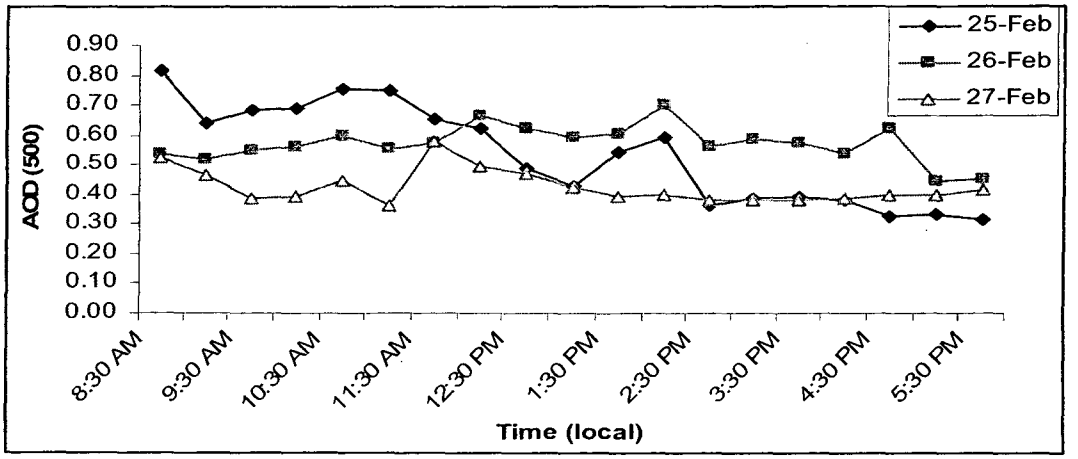

(a)

Fig: 3.3.1 Diurnal Variation of AOD (500) for different days over JNU.

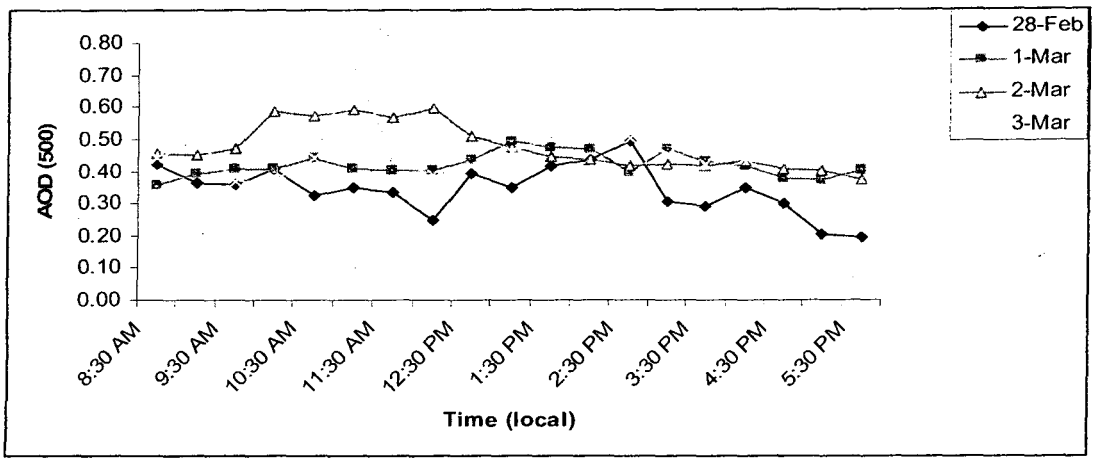

(b)

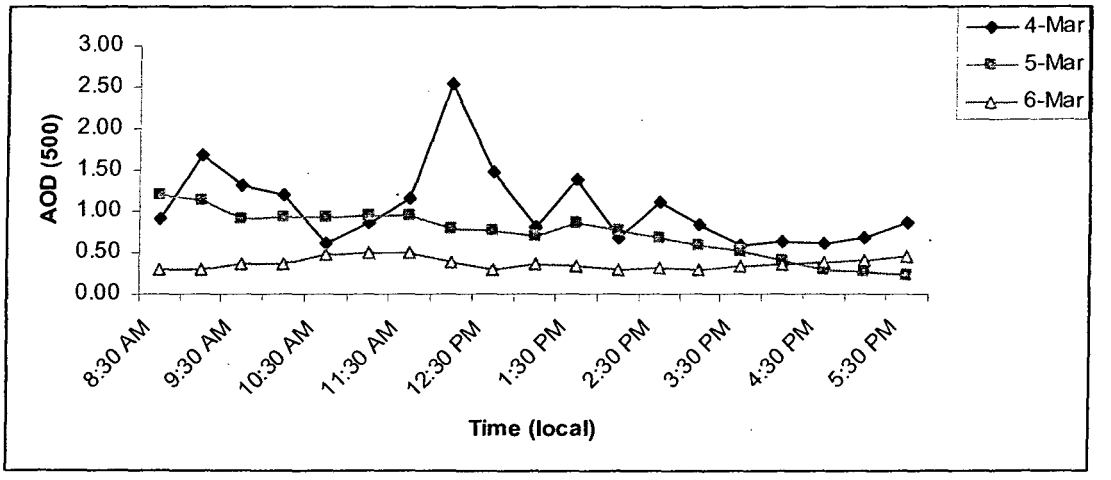

(c)

Fig: 3.3.1 Continued.....

A very different picture of diurnal variation of AOD (500) was observed on 4th and 5th March (Fig: 3.3.1c). Different high peaks during day on 4th march attributed to the presence of dust storms along with some scattered clouds. On 5th March AOD (500) decreases through out the day from morning to evening may be due to dispersion of dust storm. Very low AOD (500) values through out the day on 6th March as compared to 4th and 5th March strengthened the fact that there was slow dispersion of dust storm from morning to evening on 5th March.

The diurnal variation of α for different days over JNU is plotted in Fig: 3.3.2. It can observed that normally everyday, α increases during forenoon followed by a slight

decrease during 12 to1:30 pm which again increase during 1:30 to 2:30 pm and finally it decreases as evening progresses (except 4th and 5th March). The diurnal variation of α is coupled with AOD (500) (Fig: 3.3.3) which clearly show the dominance of small particles during 10 am to 12pm and 1 to 2:30 pm. The dominance of small particles (high values of AOD (500) > 0.4), point towards, that the aerosol loading may be due to vehicular emission from near by areas (winds coming from NNE direction to the study area). 1st March (Sunday) shows a slight increase in α value during evening due to the increase in vehicular emissions. However, 3rd March shows high value of α during whole afternoon. This result may be attributed to heavy vehicular and industrial emission.

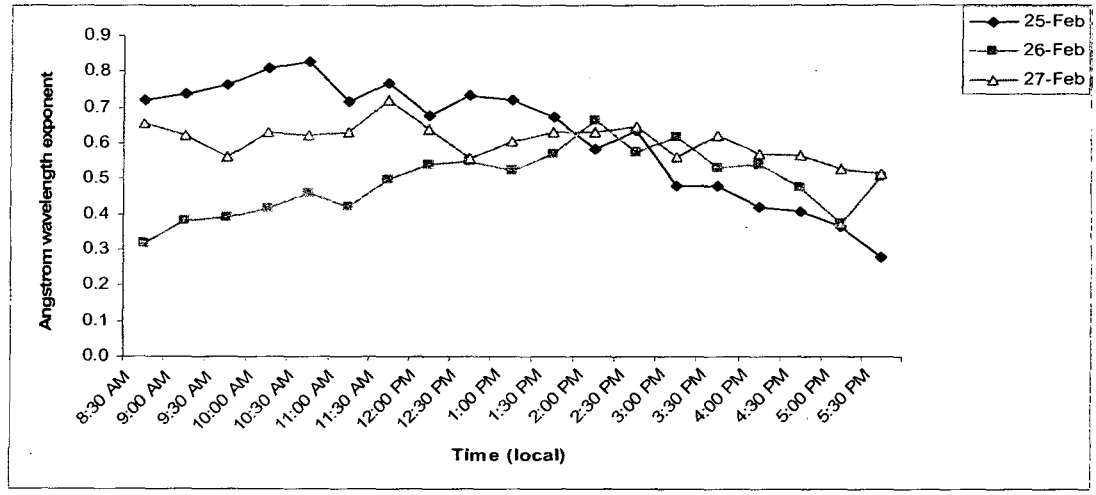

(a)

Fig: 3.3.2 Diurnal variation of Angstrom wavelength exponent (α) for different days over JNU.

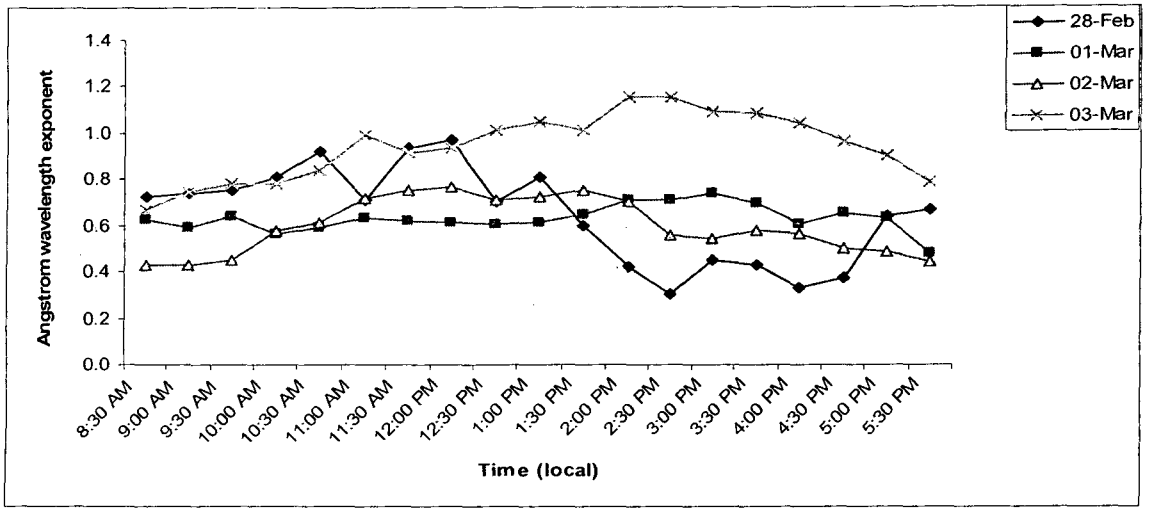

(b)

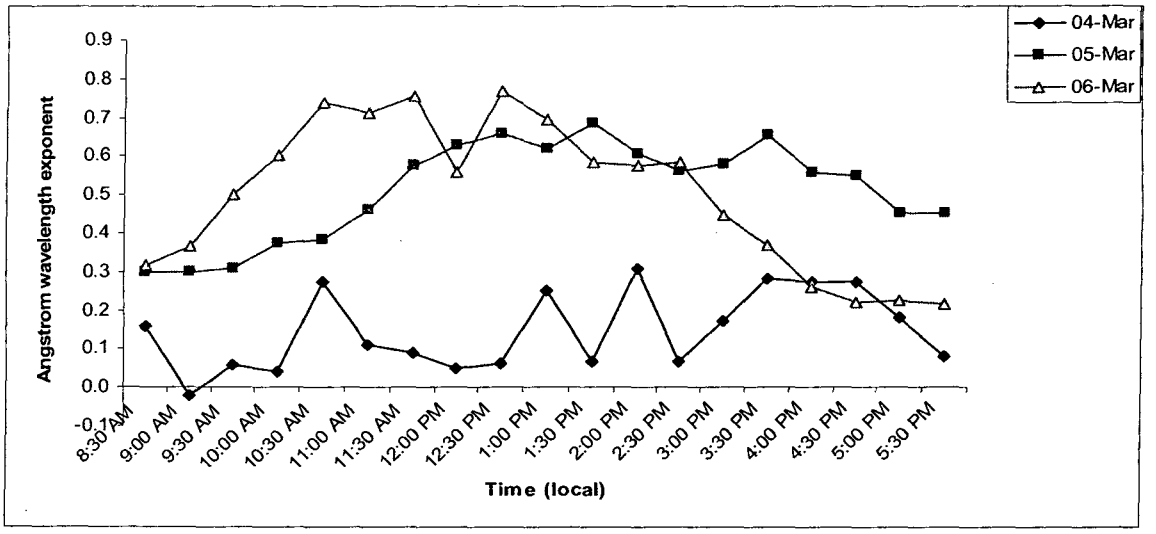

(c)

Fig: 3.3.2 Continued.....:.

The diurnal variation of a on 4th march clearly shows that the relatively lesser values of a (negative value at 9 am) fluctuating through out the day. This result also strengthened the dust storm event on this day. On 5th march a increased from morning to evening which clearly indicates the dispersion (removal) process of storm as the day progressed.

Generally, two types of relationship that have been noticed between a and AOD (500) through out the day on different days over JNU (Fig: 3.3.3). One, during morning

upto 11 am α shows a direct relation with AOD (500) i.e. increase with increase in AOD (500) and decrease with decrease in AOD (500). Second, α shows an inverse relation with AOD (500), i.e. increase with decrease in AOD (500) and vice-versa, for rest of the day. 1st and 4th March show an inverse relation between AOD (500) and α during whole day of observation, whereas, on 5th March morning's observation associated with inverse relation between AOD (500) and α, followed by a direct relation.

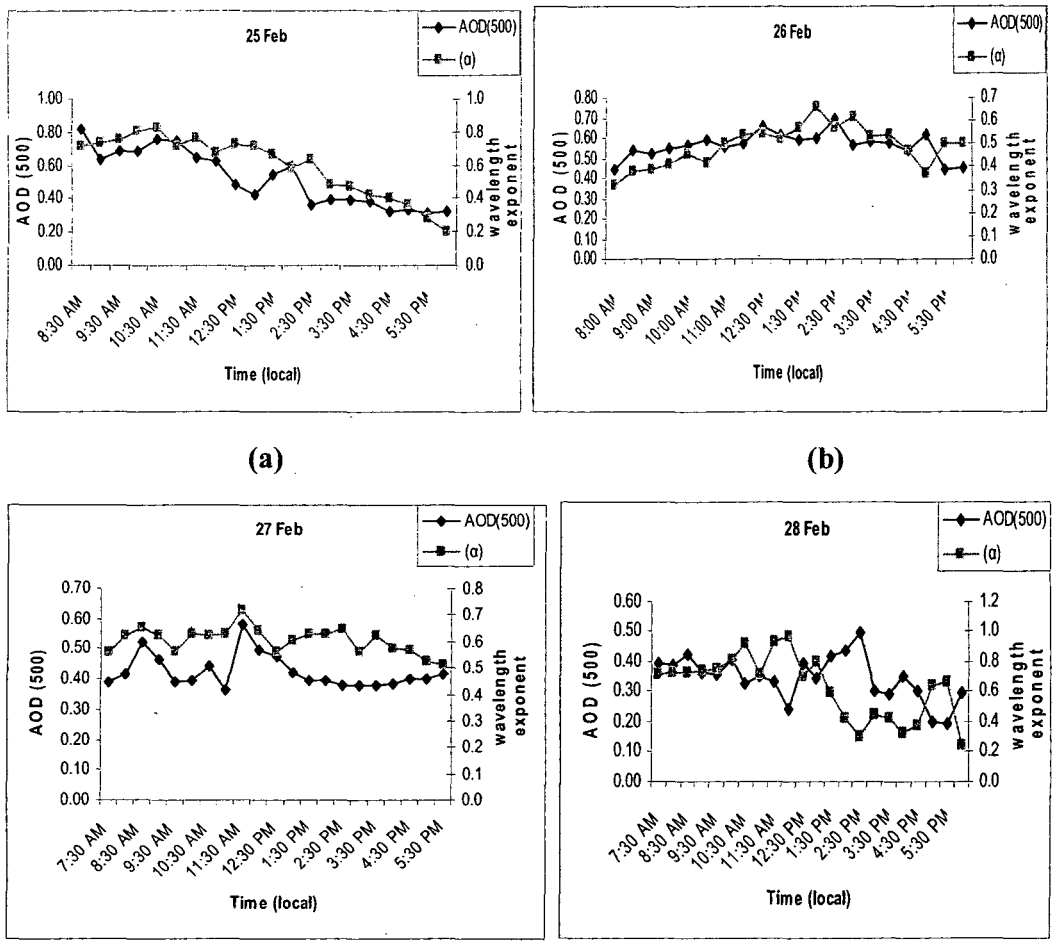

(a) (b)

(c) (d)

Fig: 3.3.3 Diurnal association between wave α and AOD (500) for different days over JNU.

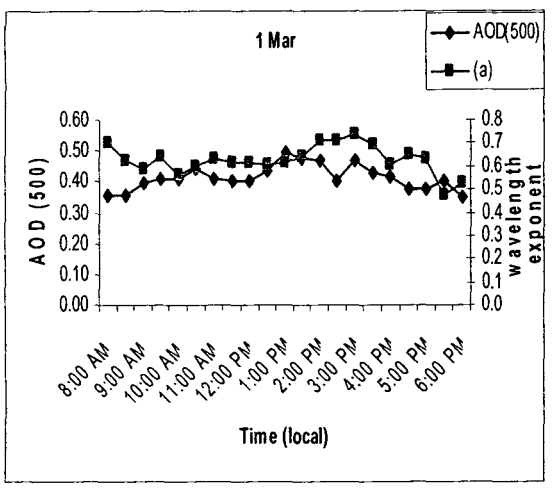

(e)

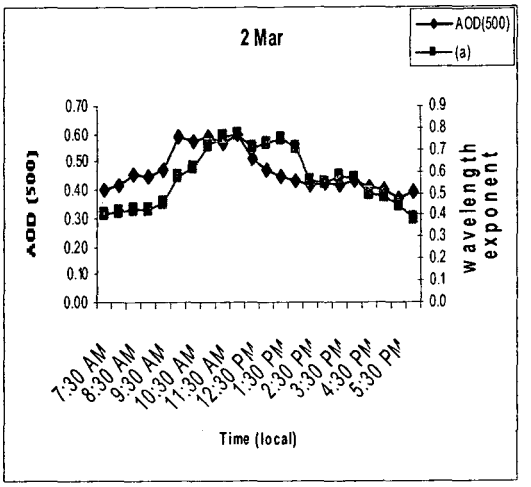

(f)

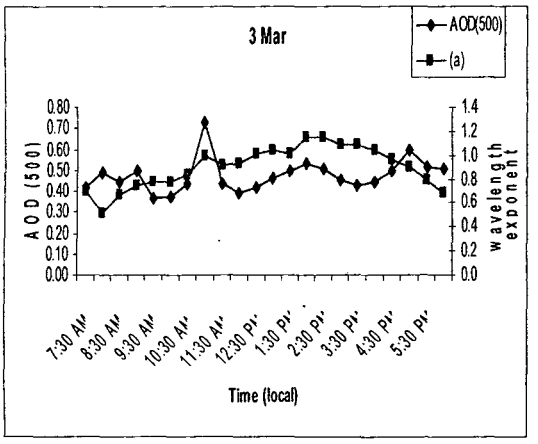

(g)

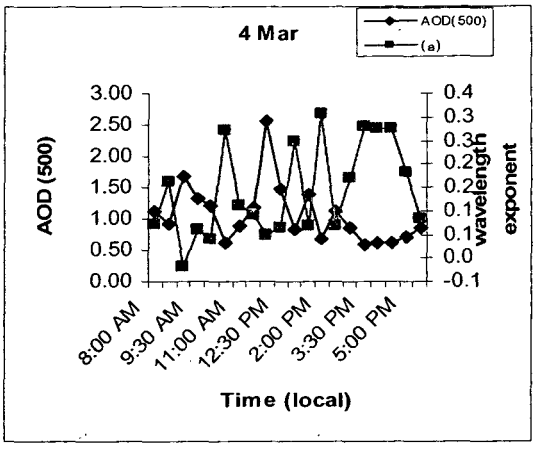

(h)

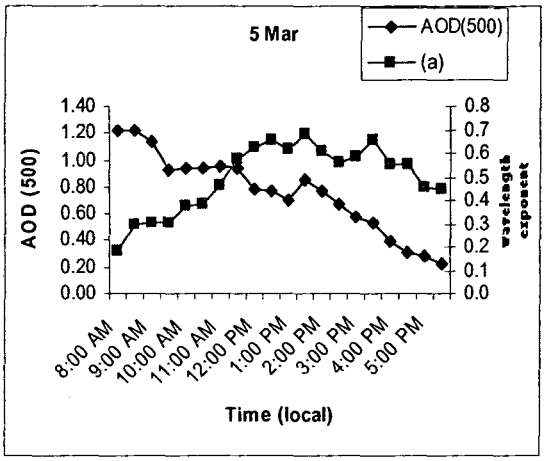

(i)

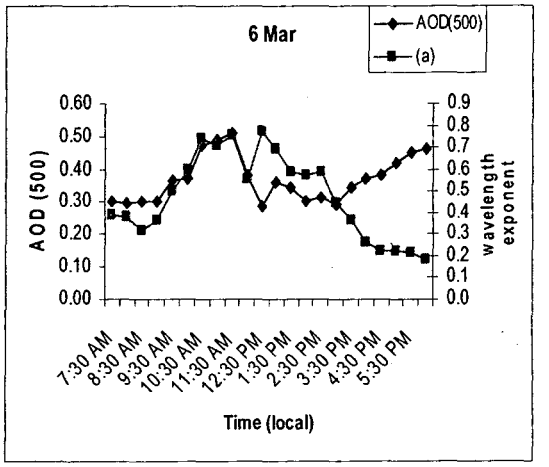

(j)

Fig: 3.3.3 Continued.....

The relationship of diurnal variation of AOD (500) and α with synoptical meteorological conditions can be inferred from comparison of Fig: 3.3.3 with Fig: 3.3.4. Normally in all observations, high AOD (500) values is associated with lower wind speed and lower AOD (500) with higher wind speed coming from NNE direction. However the days associated with high wind speed (> 15km/h) do not show any definite pattern of relationship between AOD (500) and wind speed. The AOD (500) variation with relative humidity normally do not show any definite pattern through out the day. The diurnal variation of α shows a good inverse relation with relative humidity during day time attributed to hygroscopic nature of aerosol particles present in atmosphere (expect 4th and 5th March).

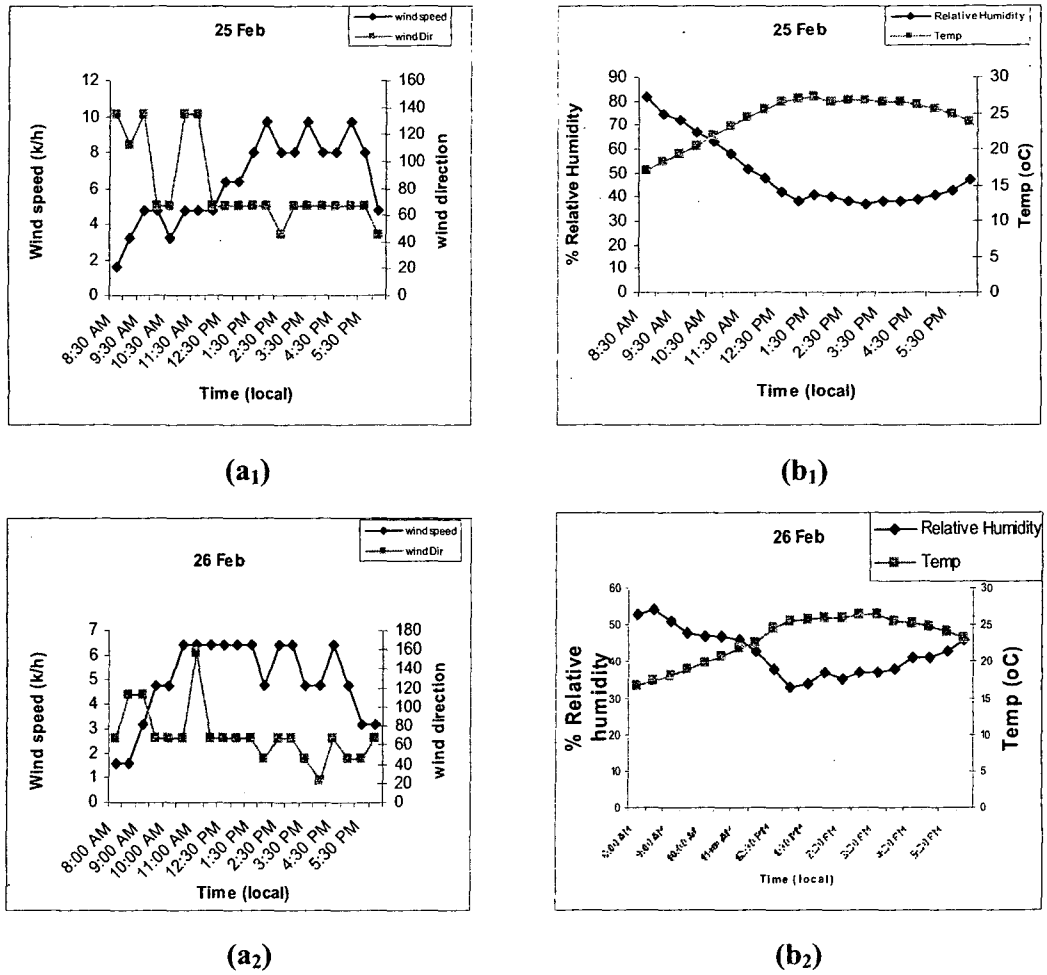

Fig: 3.3.4 Diurnal variation of meteorological parameters (wind speed, wind direction, relative humidity and temperature) for different days over JNU.

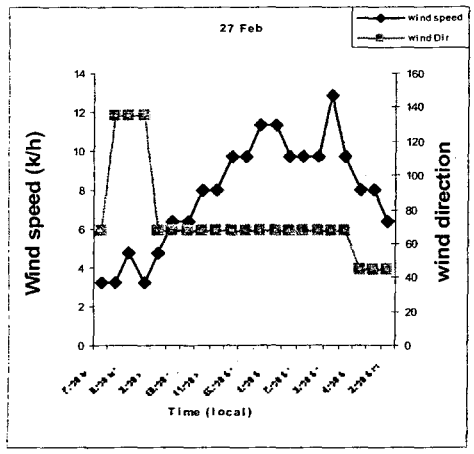

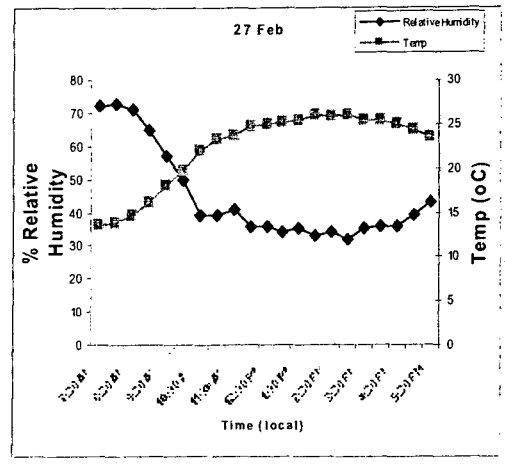

(a_3) **(b_3)**

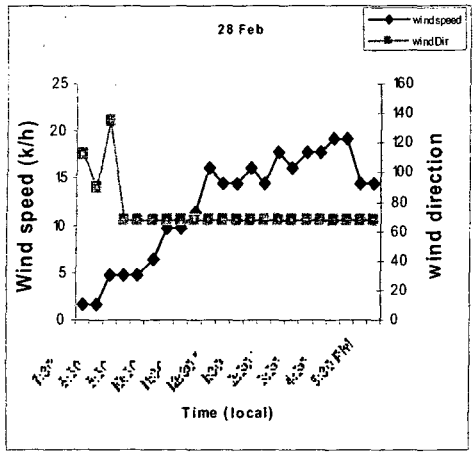

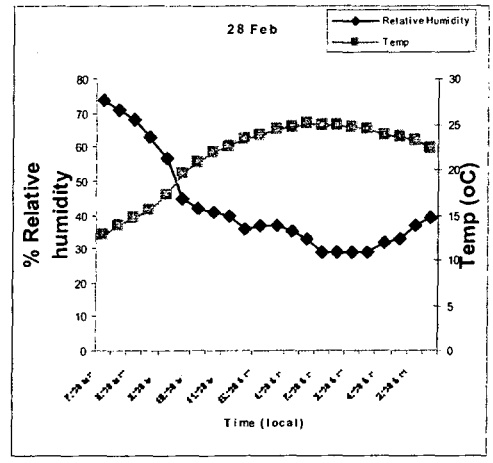

(a_4) **(b_4)**

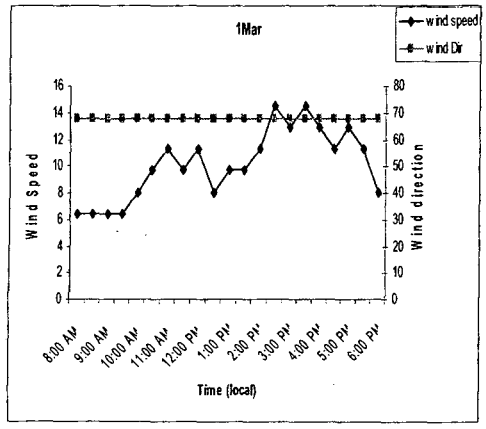

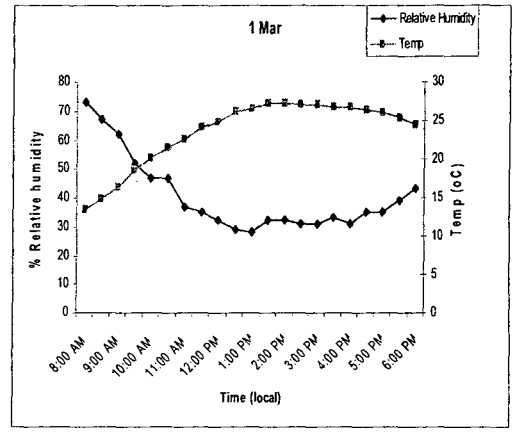

(a_5) **(b_5)**

Fig: 3.3.4 Continued.....

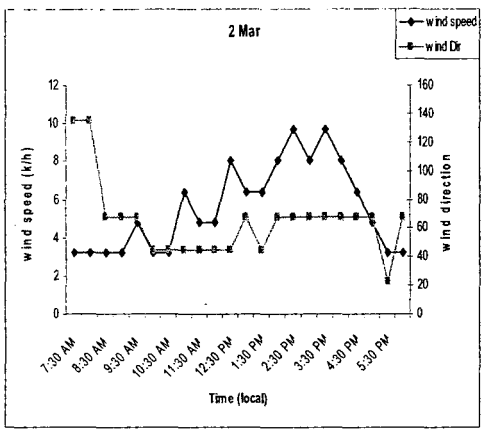

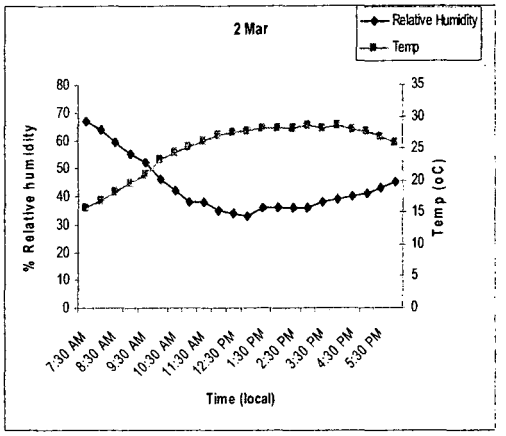

(a_6) **(b_6)**

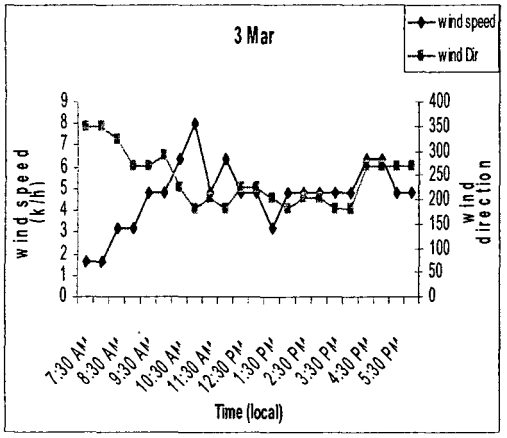

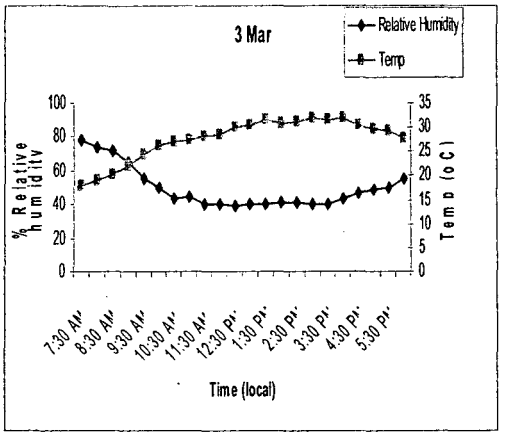

(a_7) **(b_7)**

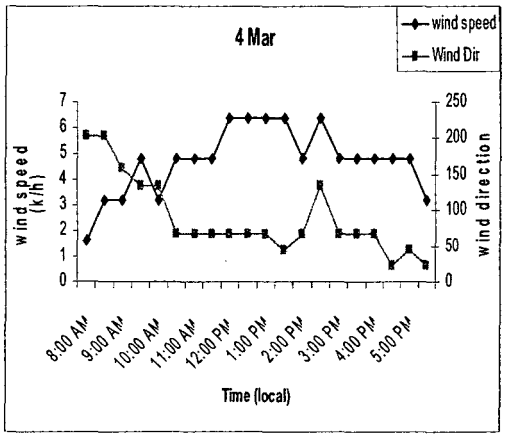

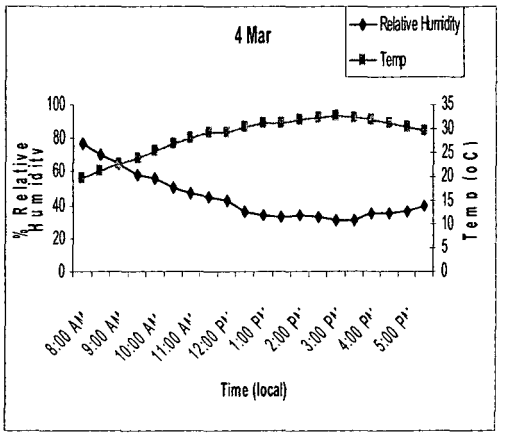

(a_8) **(b_8)**

Fig: 3.3.4 Continued.....

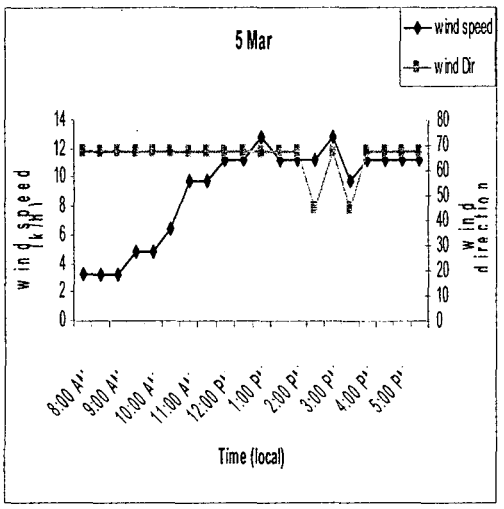

(a_9)

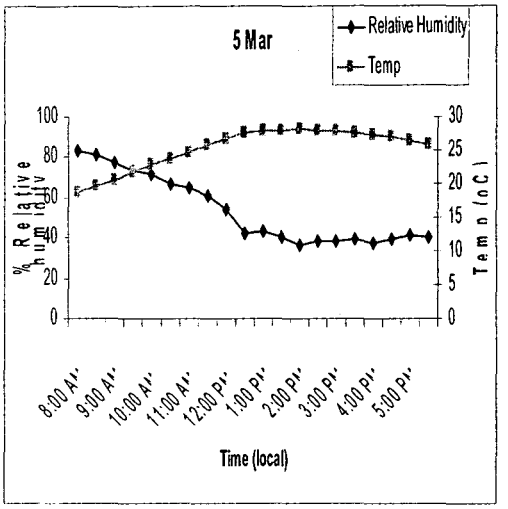

(b_9)

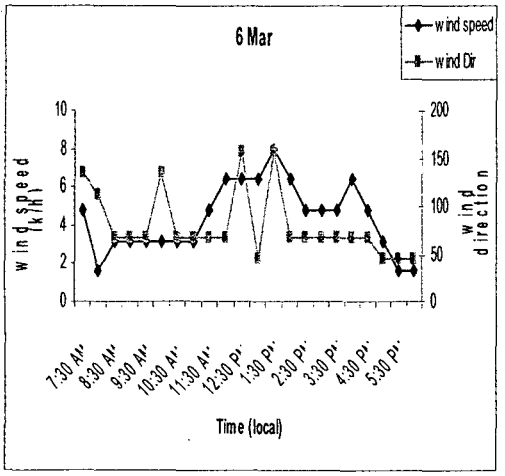

(a_{10})

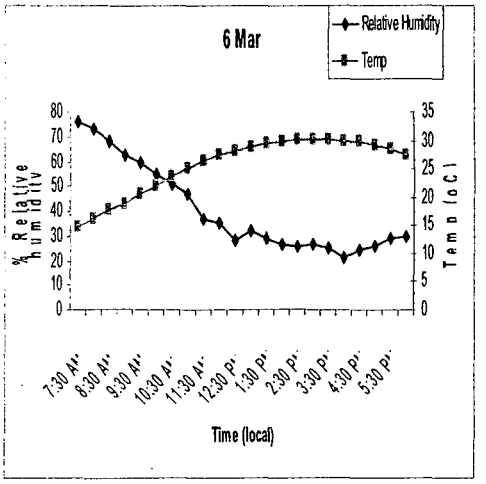

(b_{10})

Fig: 3.3.4 Continued.....

3.4 Daily variation of columnar number size distribution of aerosol

The wavelength dependant AOD values have been used to derive columnar aerosol size distribution using the inversion technique proposed by King et al. (1978). The retrieved aerosol size distribution represents an average on entire atmospheric column. Fig: 3.4.1, 3.4.2, and 3.4.3 show daily variation of columnar number size distribution over JNU, Mukherjee Nagar and Patel Nagar respectively. Instead of number of aerosols $n_c(r)$, the size distribution results are presented in terms of $dN_c/dlnr$. $dN_c/dlnr$ is representing the number of particles per unit area per unit log radius interval in atmospheric vertical column. Daily mean variation of aerosol size distribution over all sites exhibits power law size distribution i.e. Junge distribution.

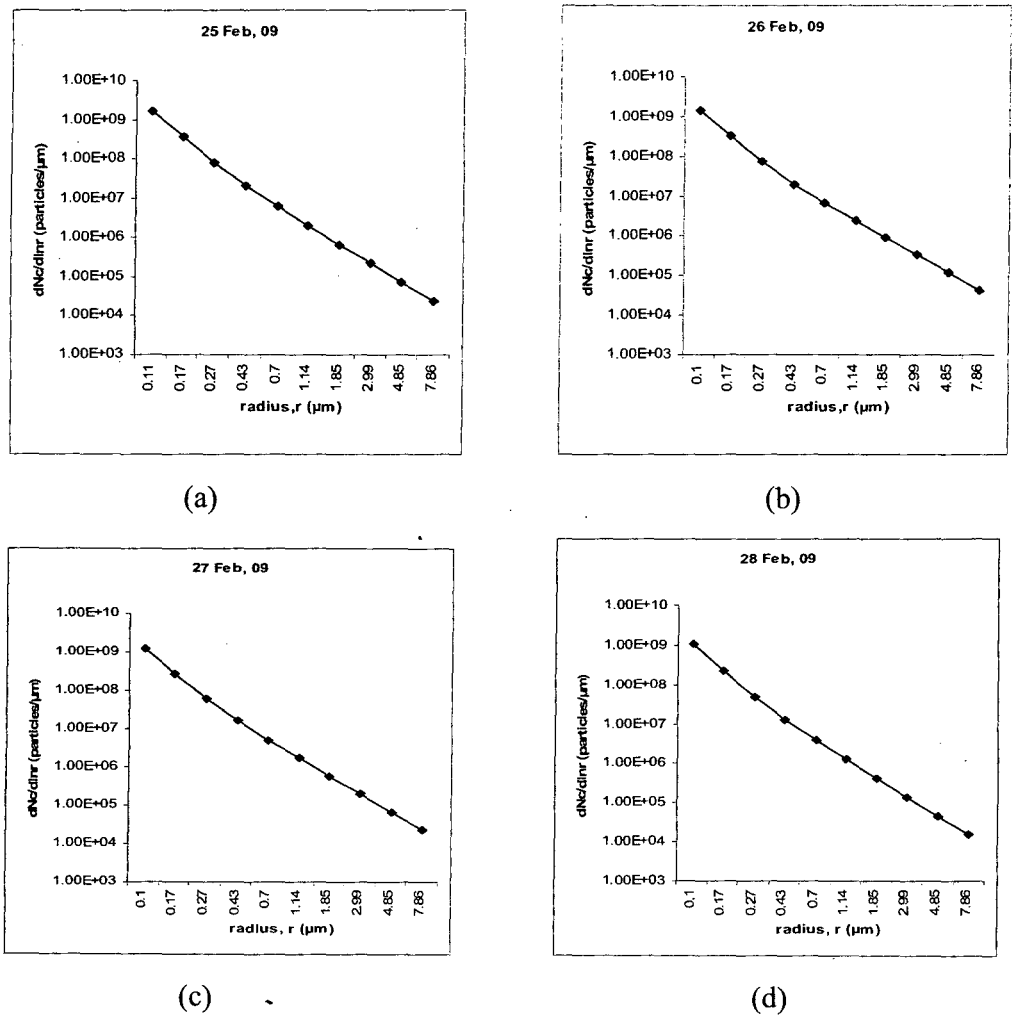

Fig: 3.4.1 Columnar number size distribution of aerosol over JNU, Delhi.

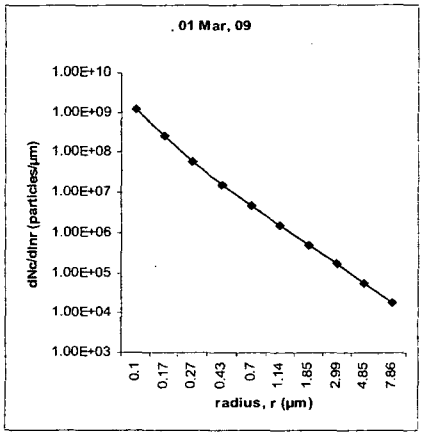

(e)

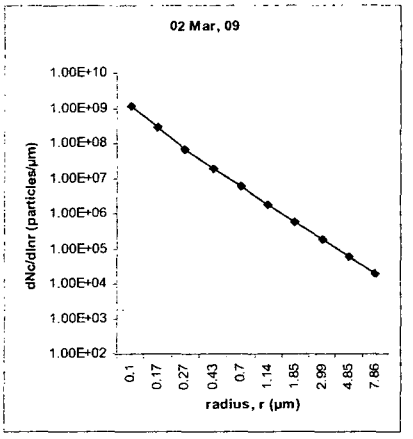

(f)

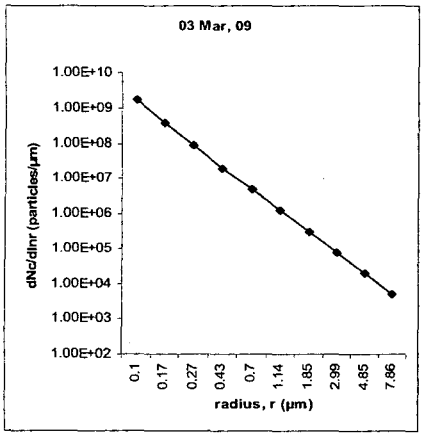

(g)

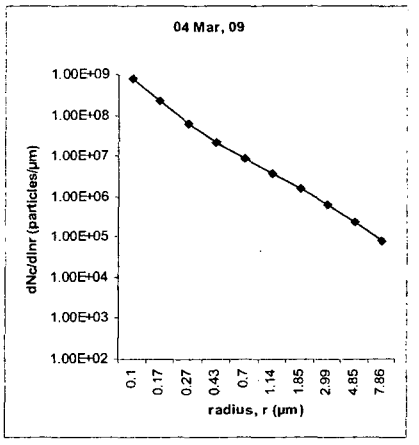

(h)

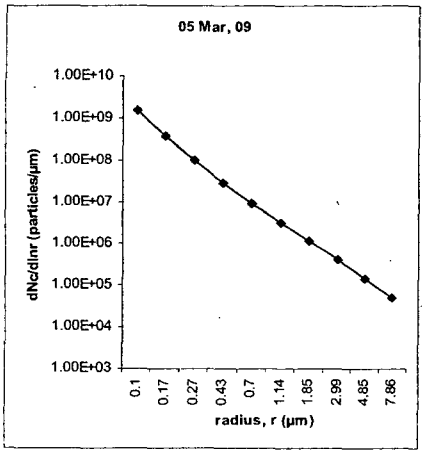

(i)

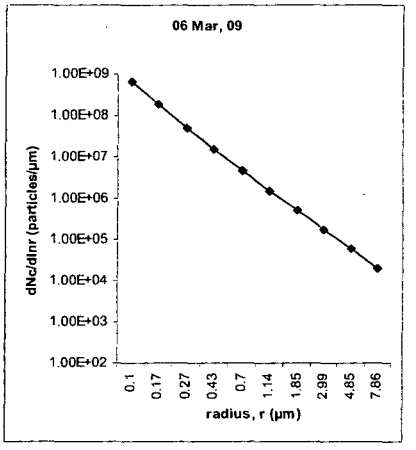

(j)

Fig: 3.4.1 continue.....

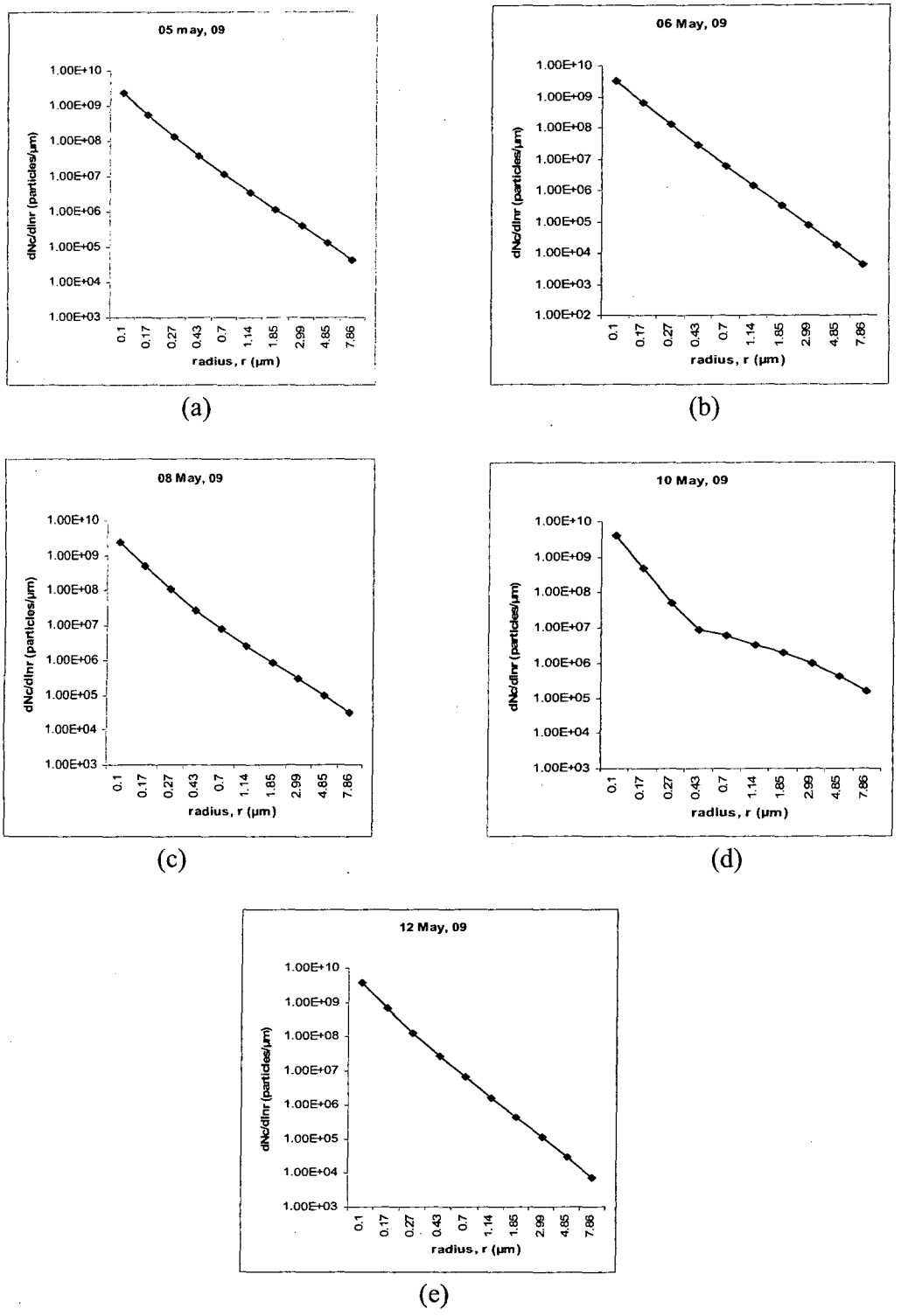

Fig: 3.4.2 Columnar number size distribution of aerosol over Mukherjee Nagar, Delhi.

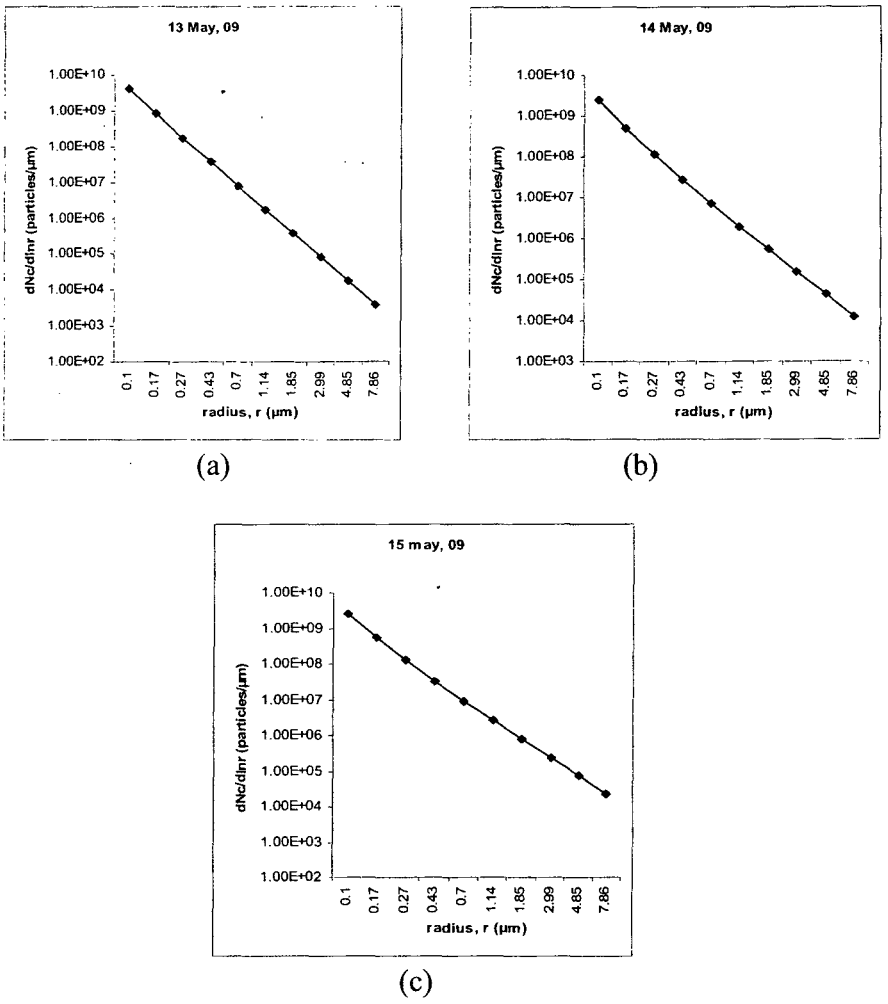

Fig: 3.4.3 Columnar number size distribution of aerosol over Patel Nagar, Delhi.

Although, all columnar aerosol number size distribution curves show power law (Junge distribution), but the equations of the curves differ significantly (chart: 3.1) from each other.

These equations represent power curve fitting of number size distribution. High regression coefficient (R^2) values indicate the perfect fitting (Table: 3.1). To calculate fine mode fraction and coarse mode fraction in aerosol, we used a general equation for number size distribution curve as follows.

$$dN_c/d\ln r = a + b\, r^{-c} \qquad (1)$$

where a, b and c are constant and vary with day specifications (Table: 3.1). We have chosen $0.1 < r < 2.5$ µm radius range for fine mode particles and $2.5 < r < 7.8$ µm radius

range for coarse mode particles. We can rearrange equation (1) in terms of total number of particles as follows.

Table: 3.1 Equation of Number Size Distribution Curve with R^2 values at three observation sites.

Site	Date	Equation of Number Size Distribution Curve	R^2 Values
JNU	25 Feb	$dN_c/dlnr = 10^7+9\ r^{-4.8763}$	0.9396
	26 Feb	$dN_c/dlnr = 10^5+9\ r^{-4.5647}$	0.9483
	27 Feb	$dN_c/dlnr = 10^5+9\ r^{-4.7767}$	0.9419
	28 Feb	$dN_c/dlnr = 10^4+9\ r^{-4.8871}$	0.9411
	01 Mar	$dN_c/dlnr = 10^5+9\ r^{-4.8613}$	0.9371
	02 Mar	$dN_c/dlnr = 10^5+9\ r^{-4.8024}$	0.9292
	03 Mar	$dN_c/dlnr = 10^1+10\ r^{-5.5797}$	0.9161
	04 Mar	$dN_c/dlnr = 10^3+9\ r^{-3.954}$	0.9374
	05 Mar	$dN_c/dlnr = 10^6+9\ r^{-4.5028}$	0.9369
	06 Mar	$dN_c/dlnr = 10^3+9\ r^{-4.5664}$	0.9249
Mukherjee Nagar	05 May	$dN_c/dlnr = 10^1+10\ r^{-4.7766}$	0.9318
	06 May	$dN_c/dlnr = 10^2+10\ r^{-5.9337}$	0.9164
	08 May	$dN_c/dlnr = 10^1+10\ r^{-4.9148}$	0.9418
	10 May	$dN_c/dlnr = 10^6+9\ r^{-4.2794}$	0.9848
	12 May	$dN_c/dlnr = 10^2+10\ r^{-5.7431}$	0.9282
Patel Nagar	13 May	$dN_c/dlnr = 10^4+10\ r^{-6.0877}$	0.9104
	14 May	$dN_c/dlnr = 10^1+10\ r^{-5.3399}$	0.9265
	15 May	$dN_c/dlnr = 10^1+10\ r^{-5.0901}$	0.9310

$$N_c = \int_{ra}^{rb} dN_c = \int_{ra}^{rb} \frac{dNc}{d\ln r} \cdot dlnr \qquad (2)$$

Where, *Nc* is total number of particles and r_a and r_b are lower and upper radius limit respectively.

$$Nc = \int_{r_a}^{r_b} \frac{dNc/d\ln r}{r} dr \qquad (3)$$

$$\text{So, total number of fine mode particles} = \int_{0.1}^{2.5} \frac{dNc/d\ln r}{r} dr \qquad (4)$$

$$\text{Total number of coarse mode particles} = \int_{2.5}^{7.8} \frac{dNc/d\ln r}{r} dr \qquad (5)$$

Now, using equation (4) and (5), we can calculate fine mode particles and coarse mode particles for different days, over all three sites. Fig: 3.4.4, 3.4.5, and 3.4.6 show fine mode fraction (FMF) and coarse mode fraction (CMF) in aerosols for different days over JNU, Mukherjee Nagar and Patel Nagar respectively.

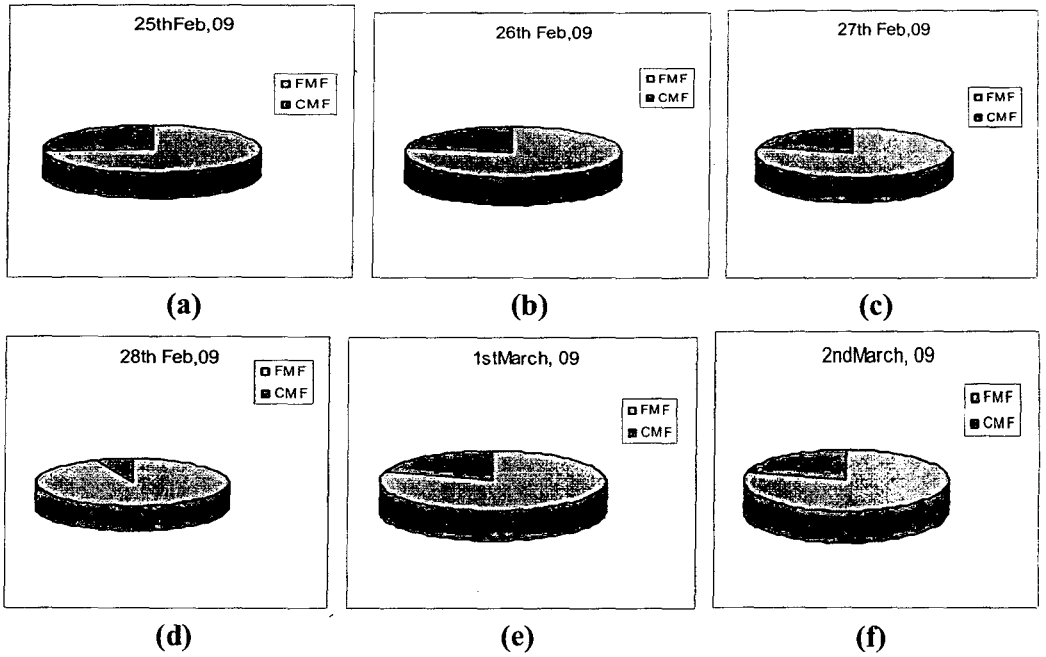

Fig: 3.4.4 Fine Mode Fraction (FMF) and Coarse Mode Fraction (CMF) in aerosols for different days, over JNU

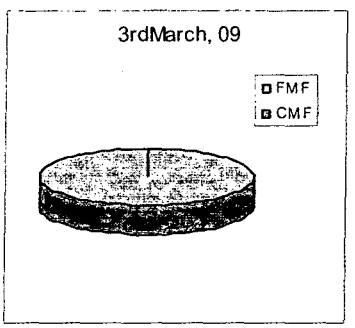

(g)

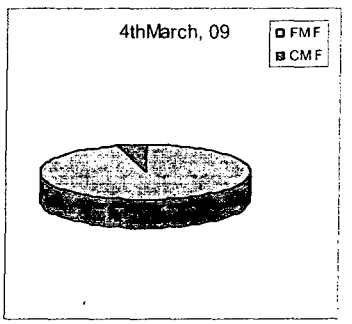

(h)

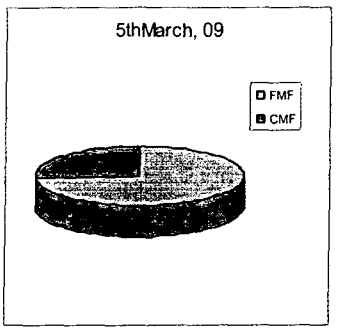

(i)

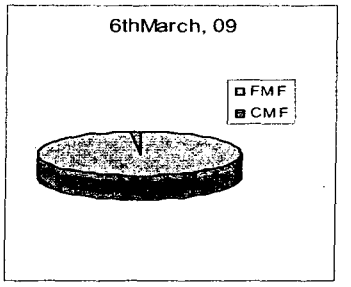

(j)

Fig: 3.4.4 continued.....

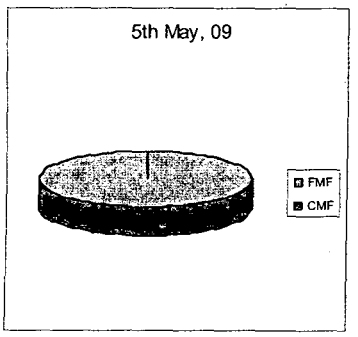

(a)

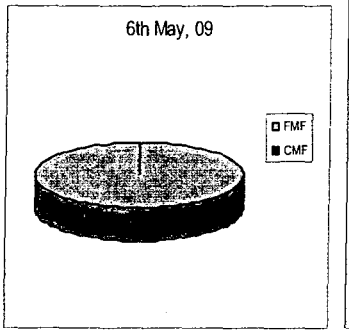

(b)

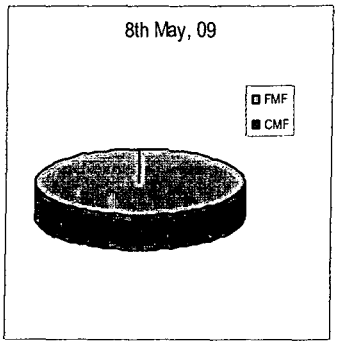

(c)

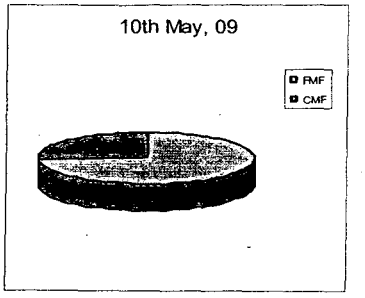

(d)

Fig: 3.4.5 FMF and CMF in aerosols for different days, over Mukherjee Nagar

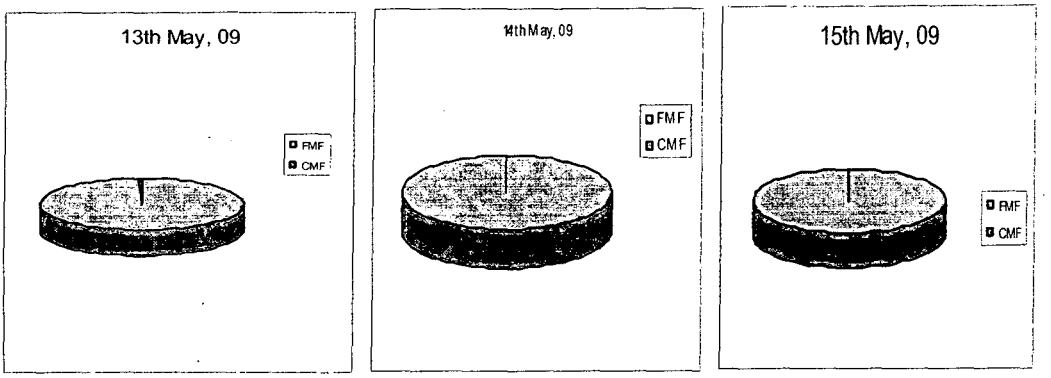

(a) (b) (c)

Fig: 3.4.6 FMF and CMF in aerosols for different days, over Patel Nagar

From Fig: 3.4.7, it is clear that almost each day at JNU, fine mode fraction (FMF) has over dominated, whilst on 3rd, 4th and 5th March, the contribution of CMF is negligibly small. As presented in section 3.2 that the low AOD (500) and low β values indicate low aerosol concentration on 3rd March. This infers the presence of only accumulation mode ($0.1 < r < 1$ μm) particles because of high FMF. Whereas, on 4th March, high AOD (500) and high β values (section 3.2) with relatively high FMF (Fig: 3.4.7), indicates presence of both, dust storm and anthropogenic aerosols over JNU. Interestingly on 6th March, low AOD (500) and low β values and moderate α value (section 3.2) coupled with dominated fine mode fractions (Fig: 3.4.7) points towards the dispersion process of dust aerosol which was observed on the previous day i.e. 5th March.

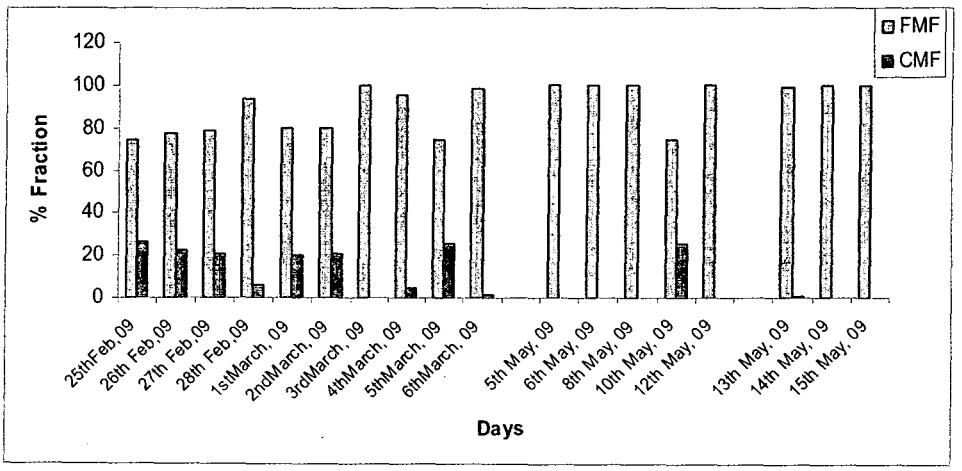

Fig: 3.4.7 FMF and CMF in aerosols for different days, for various days over Delhi.

About 99% of fine mode fraction of aerosol are observed on 5^{th}, 6^{th} and 8^{th} May (Fig: 3.4.5) which is attributed to aerosol genesis by the local vehicular and other anthropogenic emissions over Mukherjee Nagar. However, relative more coarse particles with high AOD (500) and high β values clearly indicate the occurrence of dust storm.

High fine mode fraction (about 99%) aerosols over Patel Nagar (Fig: 3.4.6) with high AOD (500) and high β values are attributed to the presence of haze layers. These haze layers may be formed by both anthropogenic emissions of near by small scale industries and fine mode dominated dust particles coming from south west direction.

CHAPTER 4

CONCLUSION

CHAPTER 4

CONCLUSION

From the present study, the following important conclusions can be drawn:

1. The spectral variation of columnar AOD, observed on different days, over all three sites, indicates a systematic spectral dependence according to classical Mie scattering theory. The magnitude of AOD decreases with increase in wavelength on each day of observation. This indicates the particle size distribution from smaller to larger size range in decreasing order.

2. An interesting feature observed from the study is that the standard deviation of AOD at each wavelength decreases towards higher wavelengths, which shows the sensitivity of AOD measurements at lower wavelengths in the visible region.

3. The magnitudes of AOD, at all wavelengths, are significantly higher over Mukherjee Nagar and Patel Nagar as compared to JNU. This may be attributed to the fact that JNU is located far away from any industrial activities as compared to the other two observed sites.

4. Over JNU, during 25 Feb-6 March, the magnitude of AOD (at 500 nm) values are in the range of 0.33 to 0.76, whereas, Mukherjee Nagar and Patel Nagar, during 5-15 May, show high values of AOD (at 500 nm) in the range of 0.65 to 0.98. This result corroborates with the fact that dust activity is found to peak in the Indian subcontinent, during spring.

5. Over JNU, 4^{th} and 5^{th} March show higher AOD (500) (0.71 and 0.76 respectively) values as compared to other days. This result shows high aerosol loading on these two days, either due to local anthropogenic activities or long range transportation of polluted aerosols. Over Mukherjee Nagar and Patel Nagar, relatively higher AOD (500) on 5^{th}, 10^{th}, and 13^{th} May (0.92, 0.98 and 0.91 respectively) is attributed to presence of haze layers during observation.

6. Our results indicate an inverse relationship between wavelength exponent α and turbidity parameter β values over all sites, except Patel Nagar.

7. This study also reveals a good association of α and β with AOD (500) values. Normally turbidity parameter β increases with increasing AOD (500) values and vice-versa, whereas, wavelength exponent α decreases with increasing AOD (500) values and vice-versa (at all sites except over Patel Nagar). Both α and β show similar patterns with AOD (500) over Patel Nagar i.e. they increase with increase in AOD (500) values and vice-versa.

8. Relatively higher value of α, over Patel Nagar (0.82-1.11) and Mukherjee Nagar (0.44-1.05) than JNU (0.2-0.9), indicated the presence of relatively finer mode aerosol particles than coarse mode, over Patel Nagar and Mukherjee Nagar. The higher values of wavelength exponent α on 3rd March (0.91), 6th May (1.05), 12th May (1.01), 13th May (1.11) and 15th May (1.01) indicate the low concentration of coarse mode aerosol particles as compared to other days of observation.

9. Higher values of β on 4th March (0.61), 5th May (0.62) and 10th May (0.74) show relatively higher aerosol loading on these days as compared to other days. Whereas, low values of β over JNU (0.26-0.41) except 4th and 5th March, show relatively low columnar aerosol mass loading than at Mukherjee Nagar (0.32-0.74) and Patel Nagar (0.37-0.47).

10. The results of diurnal variation of AOD(500), showing high AOD (500) values during 10 am to 12 pm and 2 pm to 3 pm, may be attributed to morning office traffic rush hour (vehicular pollution) and school closing times (which also leads to vehicular emission) respectively. However, 28th Feb (Saturday) shows relatively high AOD (500) range during 12:30 pm to 2:30 pm which may be attributed to high vehicular emission due to half working days on Saturday. 1st march (Sunday) shows relatively high AOD (500) after 1:30 pm, attributed to the relatively high vehicular emission caused by people going for their weekly outings on Sunday afternoon.

11. Different high peaks throughout the day on 4th March may be attributed to the presence of dust storms along with some scattered clouds. On 5th March AOD (500) decreases through out the day from morning to evening, which may be due to dispersion of dust storm. Very low AOD (500) values through out the day on 6th March as compared to 4th and 5th March, reveal that there was slow dispersion of dust storm from morning to evening on 5th March.

12. The results of diurnal variation of α show that it increases during forenoon followed by a slight decrease during 12 to1:30 pm which again increases during 1:30 to 2:30 pm and finally decreases as evening progresses. The diurnal variation of α on 4th March clearly shows that the relatively lesser values of α fluctuate throughout the day. This result also supports the observation of the dust storm on this day. On 5th March α increased from morning to evening which clearly indicates the dispersion (removal) process of storm as the day progressed.

13. Generally, two types of relationships have been noticed between α and AOD (500) throughout the day on different days over JNU. First, up to 11 am, α shows a direct relation with AOD (500) i.e. increase with increase in AOD (500) and decrease with decrease in AOD (500). Second, α shows an inverse relation with AOD (500), i.e. increase with decrease in AOD (500) and vice-versa, for the rest of the day.

14. Normally in all the observations, high AOD (500) values are associated with lower wind speed, while lower AOD (500) with higher wind speed. The winds were coming dominantly through NNE sector. However, the AOD (500) variations with relative humidity normally do not show any definite pattern through out the day.

15. The diurnal variations of α show a good inverse relation with relative humidity, which may be attributed to hygroscopic nature of aerosol particles present in the atmosphere.

16. Daily mean variation of aerosol size distribution over all sites exhibits power law size distribution i.e. Junge distribution.

17. We have seen that almost each day at JNU, fine mode fraction (FMF) has over dominated, whilst on 3rd, 4th and 5th March, the contribution of coarse mode fraction (CMF) is negligibly small. Interestingly on 6th March, low AOD (500), low β values and moderate α value coupled with dominant fine mode fractions points towards the dispersion process of dust aerosol which was observed on the previous day.

18. About 99% of fine mode fractions of aerosol are observed on 5th, 6th and 8th May which is attributed to aerosol genesis by the local vehicular and other anthropogenic emissions over Mukherjee Nagar. However, relatively more coarse particles with high AOD (500) and high β values clearly indicate the occurrence of the dust storm.

19. High fine mode fraction (about 99%) aerosols over Patel Nagar with high AOD (500) and high β values are attributed to the presence of haze layers. These haze layers could be a result of both, anthropogenic emissions of near by small scale industries and fine mode dominated dust particles coming from south west direction.

REFERENCES

REFERENCES

Adamopoulos, A. D., Kambezidis, H.D., Kaskaoutis, D. G. and Giavis, G. (2007). A study of aerosol particle sizes in the atmosphere of Athens, Greece, retrieved from solar spectral measurements. *Atmospheric Research, 86, 194 - 206.*

Adeyewa, Z.D. and Balogun, E.E. (2003). Wavelength dependence of aerosol optical depth and the fit of the ångström law. *Theoratical Applied Climatology, 74, 105-122.*

Alföldy, B., Osán, J. Z., Tóth, S., Török, A. H., Jahn. C. and Emeis, S. (2007). Aerosol optical depth, aerosol composition and air pollution during summer and winter conditions in Budapest. *Science of the Total Environment, 383, 141 - 163.*

Amato, U. and Carfora, M. F. et al. (1995). Objective algorithms for the aerosol problem. *Applied Optics, 34, 5442-5452.*

Angstrom, A. (1929). On the atmospheric transmission of sun radiation and on dust in the air. *Annales Geophysicae , 11, 156-166.*

Angstrom, A. (1961). Techniques of determining the turbidity of the atmosphere. *Tellus, 13(2), 214-223.*

Aoki, K. and Fujiyoshi, Y. (2003). Sky radiometer measurements of aerosol optical properties over Sapporo, Japan. *Journal of the Meteorological society of Japan,* 81 (3), 493-513.

Baron, P. A. and Willeck, K. (1993). Aerosol fundamental's in aerosol measurement: principle, technique and application. *Van Nostrand Reinholds, New York, 8-32.*

Bryson, R. A. and Baerreis, D. A., (1967). Possibilities of major climatic modification and their implications: Northwest India, a case study. *Bull. Am. Met. Soc., 48, 136 -142.*

Cachorro, V. E., Duran, P., Vergaz, R. and Frutos, A. M. D. (2000). Columnar physical and radiative properties of atmospheric aerosol in North Central Spain. *Journal of Geophysical Research, 105, 7161-7175.*

Cachorro, V.E., Frutos, A. M. D. and Casanova, J.L. (1987). Determination of the Ångström turbidity parameters. Applied Optics, 26, 3069-3076.

Chang, H. and Biswas, P. (1992). *J. Colloid Interface Sci, 153 (1), 157-166.*

Chang, H., Lin, W. Y. and Biswas, P. (1995). An inversion technique to determine the aerosol size distribution in multicomponent systems from in situ light scattering measurements. *Aerosol Science and Technology, 22, 24-32.*

Charlson, R. J., Schwartz, S.E., Hales, J. M., Cess, R. D. et al. (1992). Climate forcing by anthropogenic aerosols. *Science,* 255, *423-430.*

Charlson, R.J., Lovelock, J.E., Andreae, M.O. and Warren, S.G. (1987). Oceanic phytoplankton, atmospheric sulfur, cloud albedo and climate. *Nature, 326, 655–661.*

Crump, J. G. and Seinfeld, J. H. (1981). A new algorithm for inversion of aerosol size distribution data. *Aerosol Science and Technology, 1 (1), 15-34.*

Dani, K. K., Maheshkumar, R. S., and Devara, P. C. S. (2003). Study of total column atmospheric aerosol optical depth, ozone and precipitable water content over Bay of Bengal during BOBMEX-99. *Proc. Indian Acad. Sci. (Earth Planet. Sci.), 112, 205-221.*

Dockery, D. W., Pope III, C. A., Xu, X., Spengler, J. D., Ware, J. H., Fay, M. E., Ferris, B. G., and Speizer, F. E. (1993). An association between air pollution

and mortality in six us cities. *The New England Journal of Medicine, 329, 1753–1759.*

Dubovik, O. and King, M. D. (2000). A flexible inversion algorithm for retrieval of aerosol optical properties from sun and sky radiance measurements. *Journal of Geophysical Research, 105, 20673-20669.*

Dubovik, O., Holben, B., Eck, T. F., Smirnov, A., Kaufman, Y. J., King, M. D., Tanre, D. and Slutsker, I. (2002). Variability of absorption and optical properties of key aerosol types observed in worldwide locations. *Journal of the Atmospheric Science, 59, 590-608.*

Eck, T. F., Holben, B. N., Dubovik, O., Smirnov, A., Slutsker, I., Lobert, J. M. and Ramanathan, V. (2001). Column-integrated aerosol optical properties over the Maldives during the Northeast monsoon for 1998-2000. *Journal of Geophysical Research,* 106, 28555-28566.

Eck, T. F., Holben, B. N., Reid, J. S., Dubovik, O., Smirnov, A., O'Neill, N. T., Slutsker, I., and Kinne, S. (1999). Wavelength dependence of the optical depth of biomass burning, urban, and desert dust aerosols. *Journal of Geophysical Research, 104, 31333–31349.*

Esposito, F., Pavere, G. and Serio, C. (2001). A preliminary study on the correlation between TOMS aerosol index and ground-based measured aerosol optical depth. *Atmospheric Environment, 35, 5093-5098.*

Fernandez, A. J., Ternero, M., Barragan, F. J. and Jimenez, J. C. (1999). Sources characterisation of airborne particle in Seveille (Spain) by multivariate statistical analysis. *I. Dojoras, 103 (4), 261-273.*

Ferri, F., Bassini, A., and Paganini, E. (1995). Modified version of chahine algorithm to invert spectral extinction data for particle sizing. *Applied Optics, 34, 5829–5839.*

Formenti, P, Winkler, H., Fourie, P., Piketh, S., Makgopa, B., Helas, G. and Andreae, M. O. (2002). Aerosol optical depth over a remote semi-arid region of South Africa from spectral measurements of the daytime solar extinction and the nighttime stellar extinction. *Atmospheric Research, 62, 11 - 32.*

Gozmi, M. (1999). Indoor air and respiratory health in preadolescent children. *Atmospheric Environment, 33, 4081-4086.*

Gupta, P.K., Garg, S.C., Jain, S.L., Singh, R. and Gera, B.S. (2005). ISRO-GBP Land Campaign- II on Aerosols at NPL, New Delhi: Preliminary Results. A report on ISRO-GBP Land Campaign-II preliminary results.

Hagen, D. E. and Alofs, D. J. (1983). Linear inversion method to obtain aerosol size distributions from measurements with a differential mobility analyzer. *Aerosol Science and Technology, 2, 465-475.*

Hansen, J., Sato, M., Ruedy, R., Lacis, A., and Oinas, V. (2000). Global warming in the twenty-first century: an alternative scenario. *Proc. Natl. Acad. Sci. U. S. A., 97, 9875–9880.*

Haywood, J. M., et al. (1997). General circulation model calculations of the direct radiative forcing by anthropogenic sulfate and fossil-fuel soot aerosol. *Journal of Climate, 10 (7), 1562–1577.*

Haywood, J. M., Francis, P., Dubovik, O., Glew, M. and Holben, B. N. (2003). Comparison of aerosol size distributions, radiative properties, and optical depths determined by aircraft observations and Sun photometers during SAFARI 2000. *Journal of Geophysical Research,* 108, SAF 7.1-7.12.

Holben, B. N., Tanre, D., Smirnov, A., Eck, T. F., Slutsker, I., Abuhassan, N., et al. (2001). An emerging ground-based aerosol climatology: Aerosol optical depth from AERONET. *Journal of Geophysical Research, 106, 12*067-12097.

Infanta, R. and Acosta, I. L. (1991). Size distribution of trace metal in Ponce, Puesto Rico air particulate matter. *Atmospheric Environment, 25, 121-131.*

Intergovernmental Panel on Climate Change (2001). Climate Change 2001: The Scientific Basis, edited by J. T. Houghton et al., *Cambridge Univ. Press, New York.*

Iqbal, M. (1983). An Introduction to Solar Radiation. *Elsevier, New York.*

Kasten, F. (1966). A new table and approximation formula for the relative air mass. *Archiv. Meteor. Geophys. Bioklim. Ser. B, 14, 206.*

Kaufman, Y. J., Gitelson, A., Karnieli, A., Ganor, E., Fraser, R. S., Nakajima, T., Mattoo, S. and Holben, B. N. (1994). Size distribution and scattering phase function of aerosol particles retrieved from sky brightness measurements. *Journal of Geophysical Research, 99, 10341-10356.*

Kedia, S. and Ramachandran, S. (2008). Latitudinal and longitudinal variation in aerosol characteristics from Sun photometer and MODIS over the Bay of Bengal and Arabian Sea during ICARB. *Journal of Earth System Science, 117 (S1), 375-387.*

Kharol, S. K. and Badarinath, K. V. S. (2007). Effect of synoptic meteorological conditions on aerosol properties over urban environment: A study over tropical urban region of Hyderabad, India. *Acta Geophysica, 55 (3), 383-397.*

King, M. D., Byrne, D. M., Herman, B. M. and Reagan, J. A. (1978). Aerosol size distributions obtained by inversion of spectral optical depth measurements. *Journal of Atmospheric Science, 35 (11), 2153-2167.*

Kobayashi, E., Uchiyama, A., Yamazaki, A. and Kohtaro, M. (2006). Application of the statistical optimization method to the inversion algorithm for analyzing aerosol optical properties from sun and sky radiance measurements. *Journal of the Meteorological Society of Japan, 84 (6), 1047-1062.*

Krishnamoorthy, K., Nair P. and Krishnamurthy, B.V. (1988). A study on aerosol optical depth at a coastal station, Trivandrum. *Indian Journal of Radio & Space Physics, 17, 16-22.*

Li, M., Frette, T. and Wilkinson, D. (2001). Particle size distribution determination from spectral extinction using neural network. *Industrial & Engineering Chemistry Research, 40, 4615-4622.*

Li, M. and Wilkinson, D. (2001). Particle size distribution determination from spectral extinction using evolutionary programming. *Chemical Engineering Science, 56, 3045-3052.*

Mallet, M., Roger, J. C., Despiau, S., Dubovik, O. and Putaud, J. P. (2003). Microphysical and optical properties of aerosol particles in urban zone during ESCOMPTE. *Atmospheric Research, 69, 73 - 97.*

Mani, A., Chacko, O. and Hariharan, S. (1969). A study of Ångström's turbidity parameters from solar radiation measurements in India. *Tellus, 21, 829-843.*

Marawska, L., Thomas, S., Jamriska, M. and Johnson, G. (1999). The modality of particle size distribution of environmental aerosol. *Atmospheric Environment, 33, 4401-4411.*

Markowaski, G. R. (1987). Improving Twomey's algorithm for inversion of aerosol measurement data. *Aerosol Science and Technology, 7, 127-141.*

Mc Cornac, B. H. (1971). Introduction to the Scientific Study of Atmospheric Pollution. *Reide Dordrent, Holland.*

Meinart, O. A., Jones, C. D. and Cox, P. M. (2005). Strong present- day aerosol cooling implies a hot future. *Nature, 435, 1187-1190.*

Muller, D., Wandinger, U. and Ansmann, A. (1999). Microphysical particle parameters from extinction and backscatter lidar data by inversion with regularization theory. *Applied Optics, 38, 1981-1999.*

Murugavel, P., Pawar, S. D. and Kamra, A. K. (2001). Size-distribution of submicron aerosol particles over the Indian Ocean during IFP-99 of INDOEX. *Current Science (supplement),* 80, *123-127.*

Nakajima, T., Tanaka, M. and Yamauchi, T. (1983). Retrieval of the optical properties of aerosols from aureole and extinction data. *Applied Optics, 22,* 2951-2959.

Ogunjobi, K. O., Kim, Y. J. and He, Z. (2003). Aerosol optical properties during Asian dust storm episodes in South Korea. *Theoretical and Applied Climatology, 75, 65-75.*

Ogunjobi, K. O. (2007). *Variability of column-integrated aerosol turbudity and radiative parameters in Sub-Saharan West Africa. Research Journal of Applied Sciences, 2 (4), 505-511.*

Ogunjobi, K. O., He, Z., Kim, K. W. and Kim, Y. J. (2004). Aerosol optical depth during episodes of Asian dust storms and biomass burning at Kwangju, South Korea, *Atmospheric Environment, 38, 1313–1323.*

Owen, M. K., Ensor, D. S. and Sparks, L. E. (1992). Airborne particle sizes and sources found in indoor air. *Atmospheric Environment, 26, 2149-2162.*

Paganini, E., Franco, T. I. and Ferri, F. (2001). Instrument for long-path spectral extinction measurements in air: application to sizing of airborne particles. *Applied Optics, 40 (24), 4261-4274.*

Parsiani, H. and Bonilla, A. (2008). Aerosol size distribution using Sun-photometer AOD data of five wavelengths and artificial neural network. *Wseas Transactions on Systems, 7 (10), 976-985.*

Penner, J. E. et al. (1994). Quantifying and minimizing uncertainity of climate forcing by anthropogenic aerosols. *Bulletin of American Meteorological Society*, 75, 375–400.

Phillips, D. L. (1962). A technique for the numerical solution of the certain integral equations of the first kind. J. Assoc. Comput. Mach., 9, 84-97.

Pillai, P. S. and Moorthy, K. K. (2004). Size distribution of near-surface aerosols and its relation to the columnar aerosol optical depths. *Annales Geophysicae, 22, 3347-3351.*

Pinker, R.T., Pandithurai, G., Holben, B.N., Dubovik, O. and Aro, T.O. (2001). A dust out break episode in Sub-Sahel West Africa. *Journal of Geophysical Research*, 106, 22923-22930.

Prasad, A. K., Singh, R. P. and Singh, A. (2004). Variability of aerosol optical depth over Indian subcontinent using MODIS data. *Journal of Indian Society of Remote Sensing, 32, cover article.*

Prospero, J.M., et al. (2002). Environmental characterization of global sources of atmospheric soil dust identified with the Nimbus 7 Total Ozone Mapping Spectrometer (TOMS) absorbing aerosol product. *Reviews of Geophysics (1), Art. No. 1002.*

Ramanathan, V., Crutzen, P. J. and Lelievld, J. et al. (2001). Indian Ocean experiment: an integrated analysis of the climate forcing and effects of the great Indo-Asian haze. *Journal of Geophysical Research-Atmosphere, 106 (D22), 28371-28398.*

Ranjan, R. R., Joshi, H. P. and Iyer, K. N. (2007). Spectral variation of total column aerosol optical depth over Rajkot: a tropical semi-arid Indian station. *Aerosol and Air Quality Research, 7 (1), 33-45.*

Reist, P. C. (1933). Introduction to aerosol science. *Macmillan Publishing Company, New York.*

Sarkar, S., Chokngamwong, R., Cervone, G., Singh, R. P. and Kafatos, M. (2006). Variability of aerosol optical depth and aerosol forcing over India. *Advances in Space Research, 37, 2153-2159.*

Satheesh, S. K., KrishnaMoorthy, K., Kaufman, Y. J. and Takemura, T. (2006). Aerosol optical depth, physical properties and radiative forcing over the Arabian Sea. *Meteorological Atmospheric Physics, 91, 45-62.*

Satheesh, S.K. and Srinivasan, J. (2002). Enhanced aerosol loading over Arabian Sea during pre-monsoon season: natural or anthropogenic? Geophysics Research Letters, 10.1029/2002GL015687.

Schmid, B., Redemann, J., Francisco, S., Eilers, J. A., Mcintosh, D. M., Longo, K., Russell, P. B. et al. (2001). Sunphotometric measurement of columnar H_2O and aerosol optical depth during the 3rd water vapor IOP in fall 2000 at the SGP arm site. *Eleventh ARM Science Team Meeting Proceedings, Atlanta, Georgia, March 19-23,* 1-9.

Schuster, G. L., Dubovik, O., and Holben, B. N. (2006). Ångström exponent and bimodal aerosol size distributions. *Journal of Geophysical Research. 111, D07207.*

Seinfeld, J.H., (1986). Atmospheric Chemistry and Physics of Air Pollution. *John Wiley, New York.*

Shaw, G. E. (1979). Inversion of optical scattering and spectral extinction measurements to recover aerosol size spectra. *Applied Optics, 18 (7), 988-993.*

Shifrin, K. S. (1995). Simple relationship between the Angstrom parameter of disperse system. *Applied Optics, 34, 4480-4485.*

Sikka, R. D. (1997). Desert climate and its dynamics. *Current science, 72 (1), 35-46.*

Singh, M., Singh, D. and Pant, P. (2008). Aerosol characteristics at Patiala during ICARB–2006. *Journal of Earth System Science, 117 (S1), 407-411.*

Singh, S., Nath, S., Kohli, R. and Singh, R. (2005). Aerosols over Delhi during pre-monsoon months: Characteristics and effects on surface radiation forcing. *Geophysical Research Letters, 32 (L13808), 1-4.*

Smirnov, A., Holben, B. N., Eck, T. F., Dubovik, O. and Slutsker, I. (2003). Effect of wind speed on columnar aerosol optical properties at Midway Island. *Journal of Geophysical Research,* 108, 1-8.

Srivastava, A. and Jain, V. K. (2003). Relationships between indoor and outdoor air quality in Delhi. *Indoor & Built Environment, 12(3), 159-165.*

Srivastava, A. and Jain, V. K. (2005). A study to characterize the influence of outdoor SPM and associated metals on the indoor environments in Delhi. *Journal of Environmental Science and Engineering, 47 (3), 222-231.*

Srivastava, A. and Jain, V. K. (2007 a). Size distribution and source identification of total suspended particulate matter and associated heavy metals in the urban atmosphere of Delhi. *Chemosphere, 68, 579-589.*

Srivastava, A. and Jain, V. K. (2007 b). Seasonal trends in coarse and fine particle sources in Delhi by the chemical mass balance receptor model. *Journal of Hazardous Materials, 144 (1-2), 283-291.*

Srivastava, A. and Jain, V. K. (2007 c). A study to characterize the suspended particulate matters in an indoor environment in Delhi, India. *Building and Environment, 42 (5), 2046-2052.*

Srivastava, A. and Jain, V. K. (2008). Source apportionment of suspended particulate matters in a clean area of Delhi: a note. *Transportation Research Part D – Transport and Environment, 13(1), 59-63*

Srivastava, A. K., Devaral, P. C. S., Rao, Y. J., Bhavanikumar Y. and Rao, D. N. (2008). Aerosol optical depth, ozone and water vapor measurements over Gadanki, a tropical station in peninsular India. *Atmospheric Research, 8 (4), 459-476.*

Subbaraya, B. H., Jayaraman, A., Krishnamoorthy, K. and Mohan, M. (2000). Atmospheric aerosol studies under ISRO's geosphere biosphere programme. *J. Ind. Geophys. Union, 4, 77-90.*

Sumanth, E.,. Mallikarjuna, I. K., Stephen, J., Moole, M., Vinoj, V., Satheesh, S. K. and Krishnamoorthy, K. (2004). Measurements of aerosol optical depths and black carbon over Bay of Bengal during post-monsoon season. *Geophysical Research Letters, 31, 1-5.*

Sun, X., Tang, H. and Yuan, G. (2007). Determination of the particle size range in the visible spectrum from spectral extinction measurements. *Meas. Sci. Technol.,* 18, 3572-3582.

Tanre, D., Kaufman, J., Holben, B. N., Chatenet, B., Karnieli, A., Lavenu, F., Blarel, L., Dubovik, O., Remer, L. A. and Smirnov, A. (2001). Climatology of dust aerosol size distribution and optical properties derived from remotely sensed data in the solar spectrum. *Journal of Geophysical Research, 106 (1), 18205–18217.*

Tegen, I., Lacis, A. A. and Fung, I. (1996). The influence on climatic forcing of mineral aerosols from disturbed soils. *Nature, 380, 419 - 422.*

Twomey, S. (1963). On the numerical solution of Fredholm integral equations of first kind by the inversion of the linear system produced by quadratue. *J. Assoc. Comput. Mach., 10, 97-101.*

Twomey, S. (1975). Comparison of constrained linear inversion and an iterative non-linear algorithm applied to the indirect estimation of particle size distributions. *Journal of Computational Physics, 18, 188-200.*

Twomey, S., Piepgrass, A. M. and Wolfe, T. L. (1984). An assessment of the impact of pollution on the global albedo. *Tellus, 36(B), 356-366.*

Vincent, J. H. (1989). Aerosol Sampling: Sciences and Practice. *John Wiley and Sons, Chichester, 390.*

Wang, P., Kent, G. S., Mccormick, M. P., Thomason, L. W. and Yue, G. K. (1996). Retrieval analysis of aerosol-size distribution with simulated extinction measurements at SAGE III wavelengths. *Applied Optics, 35 (3), 433-441.*

Xie, J. and Xia, X. (2008). Long-term trend in aerosol optical depth from 1980 to 2001 in North China. *Particuology, 6, 106-111.*

Yamamoto, G. and Tanaka, M. (1969). Determination of aerosol size distribution from spectral attenuation measurements. *Applied Optics, 8, 447-453.*

Yoon, S. and Kim, J. (2006). Influences of relative humidity on aerosol optical properties and aerosol radiative forcing during ACE-Asia. *Atmospheric Environment, 40, 4328-4338.*